1986

Central nervous system regeneration : survival of retinal ganglion cells and optic nerve in mouse following axotomy and grafting

Matthew R. Moore
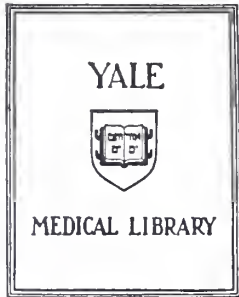*Yale University*

Follow this and additional works at: http://elischolar.library.yale.edu/ymtdl

CENTRAL NERVOUS SYSTEM REGENERATION: SURVIVAL OF RETINAL GANGLION CELLS AND OPTIC NERVE IN MOUSE FOLLOWING AXOTOMY AND GRAFTING

MATTHEW RAYMOND MOORE

1986

Permission for photocopying or microfilming of " Centr_

Nervous System F....... .on: Surv.... .

(title of thesis)

..... .d Gang.... ....s + S.... ....""...
following o ....y and ......g.

for the purpose of individual scholarly consultation or refer-

ence is hereby granted by the author. This permission is not

to be interpreted as affecting publication of this work, or

otherwise placing it in the public domain, and the author re-

serves all rights of ownership guaranteed under common law

protection of unpublished manuscripts.

(Signature of author)

Matthew R. Moore

(Printed name)

3/10/96

(Date)

CENTRAL NERVOUS SYSTEM REGENERATION:

Survival of Retinal Ganglion Cells

and Optic Nerve in Mouse

Following Axotomy and

Grafting.

A Thesis Submitted to the Yale University

School of Medicine in Partial Fulfillment

of the Requirements for the Degree of

Doctor of Medicine

by

Matthew Raymond Moore

1986

ABSTRACT

CENTRAL NERVOUS SYSTEM REGENERATION: Survival of Retinal Ganglion Cells and Optic Nerve in Mouse Following Axotomy and Grafting.

Matthew Raymond Moore

1986

Central nervous system regeneration was studied using the C57BL/6J mouse visual system as a model. The qualitative and quantitative effects of location (intraorbital, intracranial) of optic nerve transection on blood supply, ganglion cell survival, and optic axon growth was examined. Further, the comparison was made between ganglion cell survival following intracranial optic nerve transection alone versus transection and grafting of an autologous sciatic or neonatal optic nerve segment.

Data are presented which show that an intracranial transection of the optic nerve maintains ganglion cell layer blood supply whereas, intraorbital transection causes complete retinal deterioration. Cell survival was significantly increased in specific ways within the inner retinal zones of mice receiving intracranial grafts. Finally, qualitative electron micrographic evidence indicates axonal survival and attempted remyelination/ elongation at three months following intracranial transection.

ACKNOWLEDGEMENTS

I would like to express great thanks to Dr. Richard Sidman for the opportunity and resources he has made so readily available to me. I'm also grateful for his valuable constructive criticism and interest in my welfare particlarly with regard to my future residency training. My deepest thanks also to Dr. William Collins, Jr. who has been extremely helpful right from the start of my first year as both an eager advisor and genuinely fine example to me of an academic neurosurgeon. I'm in debt also to Dr. Roger Madison for our daily discussion of problems and helpful suggestions without which this project would have been very difficult. Dave Greatorex has been a key person, especially helpful in the thankless task of data collection and constantly willing to give his expert technical assistance. Many thanks to Rob Paushter for his help with data collection. I would also like to particularly thank Linda Kirschner and the rest of the staff in the Image Graphics Laboratory for their patience and essential help with the data collection and statistical programing. Bill McIntosh provided superb photographic work.

TABLE OF CONTENTS

When mammalian central nervous system axons are cut or crushed, only the initial fundamental features of a regenerative response are seen. In contrast, transection of peripheral nervous system axons (Gutman,'45; Moore,'80; Kiernan,'79; Cole,'69; Mark,'75; Engh,'72) or lower vertebrate central nervous system (CNS) fibers (Reier and Webster,'74; Murray,'76; Lanners and Grafstein,'80; Misantone et al.,'81; Murray,'82) results in extensive regrowth and functional reestablishment of target connections. Such extensive regrowth may occur in the CNS of higher vertebrates but it is often difficult to demonstrate due to the complexity of the CNS.

The rodent visual system however offers several advantages for studying regenerative growth by CNS neurons. Originating from a single cell class, the optic nerve forms a compact, isolated bundle of fibers with readily accessible parent cell body and axon (Zeman and Innes,'63; Shepard,'74). Since retinal ganglion cells are isolated from other CNS cell groups, direct application of agents via intraoccular injections can be made without involvement of other CNS constituents. The electrophysiology (Kuffler,'53; Hubel and Wiesel,'62; Wiesel and Hubel,'63; Brooks and Jung,'73), anatomical growth (Hinds and Hinds,'74; Keating, '76; Jacobson,'78; Pei and Rhodin,'70), and neurochemistry (McGeer et al.,'78; Ames and Pollen,'69; Straschill and Perwein, '75), of the normal eye and its projections are known in detail and provide the necessary basis for studying regenerative growth

in the visual system.

Early experiments reported complete ganglion cell death in mammals after optic nerve section directly behind the eye (Cajal, '28; James,'33; Eayrs,'52; Polyak,'57). Neuronal survival in other regions of the CNS has been documented if the injury takes place under certain circumstances, such as when the blood supply to the parent cell is not compromised (Bjorklund and Stenevi, '79; Madison et al.,'84) and the injury takes place at a sufficient distance from the cell body. Recent work by Aguayo and colleagues has clearly demonstrated the ability of adult rodent CNS neurons to grow lengthy axons from one region of brain or spinal cord to another when offered a segment of peripheral nerve to serve as a bridge (David and Aguayo,'81; Benfey and Aguayo, '82). Others (Kalil and Reh,'82; Reh and Kalil,'82) have demonstrated that mammalian CNS axons can regrow to some degree within the environment of undamaged CNS.

Understanding the normal sequence of events in embryogenesis may serve as a possible model for regeneration. In the mouse, the earliest retinal ganglion cell axons form within the vitreal margin of the dorsal retina on embryonic day 12 (E12) and grow toward the dorsal rim of the optic fissure. By the end of E13, fibers enter the disc area from below and form a continuous ring of retinotopically organized fascicles which completely encircle the hyloid vessel. As optic axons pass through the disc, fascicles from ventral retina are split apart at the open fissure into two bundles (nasal & temporal) which

both shift laterally, changing an annulus into a flattened plate. At E13.5 the dorsal tier of the optic stalk has pigmented neuroepithelial cells and the bottom half serves as the region for the outgrowing axons. Proximally, optic fibers develop so as to bring the early outgrowing nasal and temporal fibers together. The flattened plate of optic fascicles is then reshaped again into a marginal annulus. At E14, the stalk cell nuclei begin to migrate outward into the marginal zone. The region of the ventrotemporal retinal fibers is composed of a network of radially arranged glial cell processes separated by a "highly anastomotic system" of wide bored extracellular spaces not alligned as channels (the future optic tract). The area of the ventronasal fibers contains primitive glial cells forming a very dense "knotlike" structure with peripheral cell bodies and centripetally alligned processes (Silver,'84). Similarly arranged glia and wide bore extracellular spaces have been noted by many in regenerating CNS following axotomy. Also within transplantation and grafting experiments, as discussed in detail later, the importance of a flat linearly arranged plate of advancing fibers following surface contours has been noted.

The growth cones of developing retinal ganglion cells were found to have in vivo elongation rates of 32 microns/hour (Harris et al.,'85). In vitro growth rate on various substrates over collagen, as tried in CNS implants, has failed to achieve more than 60% of this rate. In development, growth cones are found along pial surfaces but they did not maintain adhesive contact.

Ultrastructural studies of a given neuron in embryogenesis reveals that its processes may have highly differentiated terminal arborization while still retaining growth cones on the ends of its branches (Reh and Constantine-Paton,'85). A similar structure would be hypothesized in the case of an adult fiber after axotomy with its attempted regenerative sprouting from a mature axonal trunk.

Within the developing vertebrate CNS many investigators have noted periods of naturally occuring neuronal death. There is a similarly predictable and reproducible period of cell death during abortive regeneration with sprouting processes. In the rat, retinal ganglion cell numbers follow a programed sequence of postnatal elimination: D1 200K, D3 160K, D5 143K, D10 117K, and Adult 109K (Perry et al.,'83). These studies suggest that cell death may play a role in the regular spacing of ganglion cells within the retina and in the removal of transient connections. Optic axons are all unmyelinated at D5 and only a few are myelinated at D10 (Perry et al.,'83; Sefton and Lam,'84). Interestingly, there are no gross signs of (programed) axonal degeneration since the optic nerve diameter remains unchanged. However, microscopically the decreased axonal density is equaled by individually increased axonal cross-sectional areas.

Hypotheses to explain the underlying process responsible for programed CNS cell death in development and in regeneration have been proposed. Limited physical space for efferent target connections may reduce ganglion cell number. Support for this

proposal comes from studies that show that decreasing competition through neonatal unilateral enucleation results in supranormal numbers of the contralaterally surviving ganglion cells(Sengelaub et al.,'83). Another theory suggests cell electrical activity as a determinant of retinal ganglion cell survival. Such an idea is supported by studies showing reduced cell survival following newborn intraoccular tetrodotoxin injections (Fawcett et al. ,'84). Further support for this theory comes from studies by Kierstead et al.('85). These investigators have recorded electrical activity in single regenerating rat retinal ganglion cell axons within sciatic nerve grafts after light stimuli. Their experiments support the initial presence of electro-chemical activity in sprouting axons where subsequent continued viability depends upon (correct?) synapse formation within a predetermined period. What determines this critical period or even "correct" synapse is only speculative at this time.

Neurogenesis of a functional adult visual system involves intimate interactions of neural retinal cells with nonneuronal CNS cells. Thus, a review of the embryogenesis of nonneural CNS cells is also important. During development and also following local neuronal injury, glia have been noted to release various inhibitory and growth associated proteins (Pellegrino et al.,'82; Skene and Shooter,'83). Within the rat optic nerve before D5 only two nonneuronal cell types are distinguishable, glioblasts and astrocytes. Although oligodendrocytes are not recognizable at this time period, there are many glioblasts with large nuclei.

Oligodendrocytes are seen after D5 and their maturation proceeds through a regular sequence of light, medium, and darkly staining cells. Onset of their differentiation seems to proceed in two phases with an initial signal triggering cessation of glioblast mitosis and a second inducing maturation (Valat et al.,'83). In regenerating mouse CNS, it has even been noted that oligodendrocytes start dividing before clearance of myelin debris from an injury site. Although not required the presence of axons can subsequently influence proliferation and migration of these cells (Arenella and Herndon,'83).

Early studies by Brodal ('40) reported greater sensitivity of neonatal neurons to axotomy and was called the "Gudden effect". Since the neonate is essentially within the period of neurogenesis and is believed to have greater plasticity, experiments investigating reaction to axotomy will be reviewed as a transition before the adult regeneration studies. Recently, investigators (Perry et al.,'83; Goldberg and Frank,'81; Eysel and Peichl,'85) have seen rapid axonal degeneration, increased ganglion cell loss, and lack of attempted regeneration following retinal lesions until postnatal days 20-50. Yet, contrary to these reports, Miller and Obendorfer ('81) found that the majority of neonatal rat ganglion cells survive.

The distance between axotomy and parent cell body is also thought to be an important determinant of sucessful regeneration (Lui,'54; Richardson et al.,'84; So and Aguayo,'85). Lesions made within the retina create axotomy at very short (<2mm) distances

from the ganglion cell body. Allcutt et al.('84a,b) made lesions
at greater distance from the ganglion cell body by intraorbital
optic nerve crush. Crush injuries created with forceps are
believed to differ from surgical transections in that the
resilience of blood vessels within the nerve preserves a patent
blood supply. Neonatal cells were found to be significantly more
sensitive than adult cells in magnitude of the decrease in mean
cell frequency. Large ganglion cells were particularly vulnerable
with negligible recovery months following crush. In the neonate
there was no evidence of longterm axonal regeneration although
transient collateral sprouting of cells occured.

In the adult CNS, questions of regenerative capacity have
been a longstanding interest with neuroscientists since Cajal
('28). Early studies (James,'33; Leinfelder,'38; Polyak,'41;
Kupfer,'53; Anderson,'73; Fulcrand and Privat,'77; Quigley et
al.,'77; Goldberg,'76) transecting mature optic nerve in mammals
reported retrograde degeneration with chromatolysis and near
complete dissolution of ganglion cells by 20 days post-lesion
(dpl). At 30-60 dpl large ganglion cells are rarely found in the
retina. Nearly all studies utilized an intraorbital lesion which
in the mouse may disrupt the blood supply to the retinal ganglion
cell layer (Madison et al.,'84). In studies of optic nerve
transection in adult mammals it is again important to review the
results in groups according to lesion location. Intraretinal
lesions stimulate initial vigorous sprouting characterized by
multiple bifurcations, caliber changes, and randomn fiber course

(Eysel and Peichl,'85). In these studies however, reconnection with the optic nerve and distal targets was unsuccessful. After survival of months to two years, lesioned retinas showed regions free of ganglion cells. Although neither adult nor neonate ultimately retains many injured cells, the adult triggers a regenerative sprouting which only later is aborted. After intraorbital crush in adult mouse, ganglion cell size classes were examined (Allcutt et al.,'84a,b). At 10 dpl large and intermediate cell numbers had decreased 60-80 percent, while small cell loss was 40-60 percent. With longer survival to 80 dpl the large and intermediate class decreased further to 80-100 percent as did small cells to 60-80 percent. The mean frequency of cells in the crush group in all size catagories was significantly less than in controls yet the cell area mode (30-50 sq. microns) remained constant. Some of the small cells were thought to be displaced amacrine cells whose axons were undamaged by optic nerve crush and not vulnerable to effects of this procedure. At the lesion site the majority of fibers grew for up to 20 dpl in the myelinated retinal stump then degenerated. Axons elongated within the retina and deep to the ganglion cell layer.

Misantone et al.('84) studied cell survival after adult rat optic nerve crush intracranially at the optic foramen. At one month survival they noted 50% cell size shrinkage across the range accompanied by loss of large (>90 sq. micron) neurons. Later, at 3-8 months post-crush partial recovery appears: some large neurons and size distribution approached normal. Different

from other studies, classic chromatolysis was never seen and loss of cell number occured only after an initial delay. Density of neurons in the ganglion cell layer remained normal until three months, then fell 40 percent at six months. Newly synthesized proteins decreased over the first two months and late cell loss was thought secondary to trophic loss, as discussed later under transport and trophic factors, respectively. In another study by these authors (Misantone et al.,'81), 7 days post-crush ganglion cells had decreased RNA and axonal signs of degeneration. By 14 dpl there was significant axonal loss, increased glial cytoplasm, and decreased nerve diameter. In contrast, in goldfish, where functional regeneration is effected, cells hypertrophy, RNA metabolism and axonal transport increase (Misantone et al.,'81).

Grafstein and Ingoglia('82) examined ganglion cell size and number changes after intracranial transection of adult mouse optic nerve. Three days after transection, ganglion cell number had decreased by 20 percent and cross-sectional area by 25 percent. At three months, the cell number further decreased to 50 percent but cross-sectional areas were back to normal levels. There was no unequivocal evidence of axonal regeneration at any time at the lesion site. Some surviving axons in the retinal stump showed terminal bulbs which decreased with time, suggesting impaired axonal transport. Comparing intraretinal, intraorbital, and intracranial lesions, it appears that with increasing distance from axotomy to cell body, there is greater ganglion cell survival yet decreased regenerative axonal sprouting. Some

of the variability of cell numbers among comparable studies may be due to difficulty in identifying ganglion cells from amacrine cells and to a lesser extent the clear identification of glia. Indeed, verification of these experiments in the future should be done using newly developed and highly specific monoclonal antibodies (Balkerna and Drager,'84; Akagawa and Barnstable,'84).

The studies reviewed above have attempted to describe in detail the reaction to axotomy in neonatal and adult optic nerve. The general lack of successful regeneration found by these studies results in several theories to explain regenerative failure. Nine hypotheses to explain regenerative failure are presented below without regard to any particular order of significance:

A) absence of nonneuronal cell guides for sprout elongation (Cajal,'28; David and Aguayo,'81; Benfey and Aguayo,'82; Weiss and Taylor,'46)

B) physical barricade of connective and astrocytic scar (David and Aguayo,'81; Benfey and Agauyo,'82; Reier et al.,'81; Guth et al.,'81; Windle,'56; Agauyo et al.,'81; Neuman et al.,'83)

C) local autoimmune reaction at injury and sprouting site (Sparrow et al.,'84; Berry and Riches,'74; Zalewski and Silver,'80)

D) growth termination after early synapse formation (LeGros Clark,'42a,b; Berstein and Berstein,'71)

E) differences in blood-brain and blood-nerve barrier (Kiernan,'79)

F) failure to retrogradely transport trophic factors (Misantone et al.,'84; Grafstein and Ingoglia,'82; Smalheiser et al.,'81; Redshaw and Bisby,'81)

G) toxic extracellular components and increased retrograde transport load (Grafstein and Ingoglia,'82; Pelligrino et al.,'82)

H) excessive axoplasmic and cytoplasmic volume
loss (Grafstein and Ingoglia,'82; Meiri and
Grafstein,'84)

I) inability to undergo genetic shift to exhibit
regeneration program (Hadani et al.,'84).

The actual cause of regenerative failure is likely to involve a combination of these theories. It is logical now to review "interventional" attempts to increase the regenerative response based on the acceptance of given failure theories. As a start it is believed that neural-glial cell interactions are intimately associated in order to bring about normal development, and through various trophic influences seem to have a role in CNS regeneration. Clinically, it has been demonstrated that peripheral nervous system unlike CNS, can survive axonal transection and regrow functional axons to their original targets. Rat sciatic nerve has been studied after transection and placement into various tubes (Lundborg et al.,'82; Williams and Varon,'84; Seckel et al.,'84). Regrowth progressed through stages of fluid accumulation (neuronotrophic in cell cultures), continuous coaxial fibrin matrix formation, cellular replacement of matrix, and axonal elongation/myelination. Biochemical isolation of factors effecting growth were tested in vivo. Extrapolating to CNS, whole sciatic grafts or various isolated growth associated proteins were tried. Initially, investigators noted glial reactivity and de novo synthesize of a factor called reactive glial protein (Pellegrino et al.,'82), a 37kDa soluble, acidic protein secreted from distal denervated sheath cells

(Skene and Shooter,'83). Antibodies were made to this protein in four related forms (Ignatius et al.,'84; Snipes and Freeman,'84) from adult rat optic nerve, sciatic nerve, neonatal sciatic nerve, and normal rat serum. This protein is synthesized at maximal rate 2 weeks post-lesion and continues through the fourth week. Recently, protein synthesis from nonneuronal sheath cells in injured, intact, and developing sciatic and optic nerves was examined. The 37kDa molecule was increased with denervation, the 51 and 54kDa were found in intact mature nerve sheath, and a 70kDa was present only after axotomy (Muller et al.,'85). The 37 kDa protein accumulated within adult sciatic nerve but not optic nerve, and correlates with axon growth. It has striking homology to apolipoprotein E and may play a role in assembly/maintenance of myelin or axonal membranes in development and regeneration (Ignatius et al.,'85). Similarly, a 15kDa acidic protein called glial maturation factor (Lim and Miller,'83) was isolated and found to stimulate astrocytic proliferation and differentiation.

Another group has found that implanting substances from regenerating fish optic nerve or neonatal optic nerve triggered a cell body response in adult mammalian CNS (Schwartz et al.,'84; Lavie et al.,'85; Stein-Izsak et al.,'85). This growth associated triggering factor (GATF) was a 10kDa protein from nonneuronal cells which induced synthesis of specific neuronal polypeptides and sprouting of new fibers after optic nerve injury.

The preceeding studies present evidence for a trophic influence of the nonneuronal cell environment while others

believe the target tissue itself expresses important factors. Experiments removing neonatal rat superior colliculi (Dreher et al.,'83) cause a 60 percent ganglion cell loss. As noted previously and in their controls, natural ganglion cell decline was only 35 percent. With target removal the loss occurs over the same natural time course thus supporting the importance of target tissue trophic factors.

Recently, a glycoprotein on basement membrane and cell surfaces called laminin was found to be more highly adhesive and promoted superior axonal outgrowth from retinal explants than either collagen (type I or IV) or fibronectin (Smalheiser et al.,84). This protein is synthesized in schwann cells and astrocytes. Studies filling nerve guide lumens with 80 percent laminin and extracellular matrix components induced growth of a nerve cable at 2 weeks post-lesion while controls had nothing following sciatic nerve transection (DaSilva et al.,'84; Madison et al.,'85).

Other studies of regeneration have involved trying to alter the response following lesions without using animal-derived trophic factors. Systemic administration of antimitotic AraC has been reported to inhibit gliosis following rat optic nerve crush (Politis,'85) thus providing a more supportive millieu for regeneration. Also, X-irradiation (Neuman et al.,'83) and direct calcium ionophore applicaton (Meiri and Grafstein,'84) were found to enhance regenerative capacity of goldfish retinal ganglion cells. In contrast, intraperitoneal colchicine or vincristine

sulfate (Davis and Benloucif,'81), intraoccular acetoxycyclohexi-
mide (McQuarrie,'85) and antibodies to gangliosides (Sparrow et
al.,'84) all inhibit the regeneration of goldfish optic nerve
following crush or transection.

Some investigators have emphasized the biophysical aspects
of growth in development and regeneration. Thus, the
extraneuronal environment has been examined for guides in
rectilinear elongation. In culture, retinal ganglion cell
survival and growth was greatest when plated over immature
astrocytes which are both glial fibrillary acidic protein
positive and flat in shape (McCaffery et al.,'85). As mentioned,
development seems to be along surfaces (flattened plates). Such
directed growth is also seen in grafting experiments where
uniformly, maximum labeling of ingrowing axons is seen
circumferentially. Three theories of rectilinear growth are: I)
existence of small caliber alligned extracellular matrix fibrils
(Silver,'84), II) contact inhibitory interactions between the
very earliest growing fibers maintain parallel growth (Dunn
,'71), III) greater preferential affinity between early fibers
and their glial environment than for each other (Silver,'84).
Regeneration may not be successful in adulthood because these
guiding fibrils or surface affinities of embryogenesis have
disappeared.

Similarly investigations have examined the intraneuronal
biophysics with regard to protein and transport rate changes.
Development of optic nerve is associated with a programed

sequence of induction of rapidly transported proteins in rat
ganglion cells (Bock et al.,'84). Three transport classes were
found: a large class remaining at constant rate, a second of 20
and 43kDa proteins only neonatally, and a final class of 29kDa
proteins solely in adulthood. Comparing this to axotomy in adult,
Redshaw and Bisby ('81) found that in peripheral nerves fast
axonal transport of a 23kDa protein increased relative to a 28kDa
protein. In contrast, transecting optic nerve caused no increase,
and transport activity disappeared by 4 dpl. Yet, Misantone et
al.('84) also in rat optic nerve reported transport up to 2
months post-lesion. Athwal et al.('84) saw a transient increase
at 6 dpl with decrease to 75 percent normal at 14 dpl. It is
unknown in the CNS whether transport failure is the primary event
or that it may be secondary to trophic loss or absent genetic
reinduction.

Since schwann cells may secrete trophic factors and
peripheral nerves have the capacity to successfully regenerate
over great lengths, investigators have attempted to recreate this
environment locally in CNS through nerve grafts. Grafting
experiments allow one to direct the course of sprouting axons and
then determine their source, direction, and target terminations.
From Aguayo's laboratory, studies have demonstrated extensive
elongation of CNS spinal axons (David and Agauyo,'81; Benfey and
Agauyo,'82; Richardson et al.,'84; Salame and Dunn,'84) into
sciatic nerve grafts. Regenerating fibers were frequently
ensheathed by schwann cells in their course through the graft.

The role of local environment is further demonstrated by the reverse experiments where CNS fiber tracts grafted peripherally abort or decrease the normally vigorous regrowth (Aguayo et al.,'81; Agauyo et al.,'78; Weinberg and Spencer,'79).

In grafting studies using rodent visual system as a model for CNS regeneration, it is again important to review results in groups according to axotomy to cell body distance. With short distances, So and Aguayo ('84,'85) recently presented evidence of extensive axonal sprouting and elongation when sciatic nerve was grafted intraretinally, directly through sclera without optic nerve injury. Axons of ganglion cells were thus transected in the stratum opticarum en route to the optic nerve head. Yet, within the retina there may be a factor confounding the distance variable which is related to the lack of oligodendrocytes until the optic nerve head. McConnell and Berry ('82) believe oligodendrocytes (central myelin) release axonal-growth inhibiting factor (AGIF) which normally prevents successful CNS regeneration. All intraretinal grafts contained myelinated and unmyelinated axons whose soma size histograms were similar to control animals. No cells could be doubly labelled from the graft and optic nerve thus eliminating the case of sprouting from undamaged collaterals or uninjured cells. These sciatic grafts ended blindly after running subcutaneously over the skull, thus refuting the importance of target-guided growth at least for the initial outgrowth of regenerating axons.

In experiments grafting sciatic nerve to transected optic

nerve head (Vidal-Sanz et al.,'85), ganglion cells of various
sizes throughout the retina regenerated axons the length of the
graft. Cell number and size classes were not presented.
Intraorbital graft experiments using sciatic (Politis and
Spencer,'82) and neonatal optic nerve (Hadani et al.,'84) have
shown a small proportion of myelinated axons can sprout and
elongate into grafts. Surviving ganglion cell bodies however were
not quantified.

Richardson et al. ('82) examined the retinal stump and
ganglion cell layer after intracranial optic nerve transection
and sciatic nerve grafting in the rat. At this distance, axonal
sprouting was less than 0.5 mm and not enhanced by peripheral
nerve grafts. At 2 weeks after transection, there were few axons
in the graft yet retinal architecture was reportedly preserved
with no infarction or ganglion cell loss. Retrograde axonal
degeneration was then rapid with fiber numbers near the globe
falling to less than 10 percent at four weeks.

The present study first tested the hypothesis that
inadvertent destruction of the blood supply to the ganglion cells
of the retina contributes to the commonly observed cell death,
and that maintenance of a patent blood supply allows some of
these ganglion cells to survive. The effects of optic nerve
transection with and without retention of a patent blood supply
are compared and the vascular anatomy in the mouse is examined.
The second part of the study compares the number and size class
of surviving retinal ganglion cells after: a) intraorbital, or

b) intracranial optic nerve transection, or c) intracranial transection with grafting of autologous sciatic, or heterologous neonatal optic nerve.

Intra<u>cranial</u> transection is a useful model of CNS regeneration. Intraorbital and intraretinal lesions are likely to disturb blood supply to the ganglion cell body, and axotomy within the retina, with its absence of oligodendrocytes, is not an accurate representation of the vast majority of CNS tracts to which regeneration progress will be applied.

MATERIALS AND METHODS

Optic nerves and retinas of male C57BL/6J mice from our departmental colony were examined in these studies. Before and after surgery the mice were maintained under standard controlled conditions of temperature and humidity with 12-hr on-off light cycles and were furnished mouse breeder chow (Wayne Co.) and water ad lib. Intraperitoneal injection of Avertin anesthesia (0.5g tribromoethanol dissolved in 0.25g 2-methyl-2-butanol and 19.5 ml water) was used for all operative procedures.

Optic nerve transection and grafting

Intracranial exposure of a 2 mm segment of the right optic nerve midway between the optic chiasm and foramen was attained through a small craniotomy just anterior to the coronal suture overlying frontal cortex. After opening dura mater, careful aspiration and hemostasis of underlying cortex and subcortical structures within a rostrally oriented path along the temporal bone was performed. Upon reaching basal dura, the pial plexus of capillaries and the anterior cerebral artery was gently retracted medially. Using fine microscissors, the optic nerve was completely transected perpendicular to its axis after gentle elevation into the open blades. A microhook was then passed through the transection to insure total axotomy. In the group receiving intracranial transection alone (N=4), the nerve stumps

were realigned _en_ _face_ into their original position with replacement of overlying pia and arteries using minimal direct handling. The entry cavity was filled loosely with Gelfoam (Upjohn) and the wound closed.

In the group receiving an intracranial graft (N=7), the approach was identical but now required two transections 1 mm apart in order to remove a segment of adult optic nerve. The gap was immediately filled by an equal length of autologous sciatic nerve (from the hip region) removed at the time of optic nerve exposure. Longitudinal fiber orientation was maintained and nerve stump faces gently apposed without sutures to minimize local trauma and scarring. Similarly, in some animals a segment of neonatal day 1 mouse optic nerve was used to bridge the intracranial gap. The closure was as described previously.

For intraorbital transection (N=4), the right eye was rotated medially and the lateral canthus and limbus were opened to reveal the extraocular muscles. Lateral and superior rectus muscle were cut allowing the fat and Tenon's capsule to be retracted laterally exposing the optic nerve. Using microscissors the nerve was carefully transected perpendicular to its course and hemostasis maintained at 1 mm behind the globe. The orbital contents were then released and the eye returned to its normal rotation thus closing the lateral incision. This surgical manipulation severs the optic nerve as well as the ophthalmic artery, thus compromising blood supply to the retina while retaining perfusion to other orbital components.

Blood supply

The retinal and optic nerve blood supply was assessed in 14 mice either before or after optic nerve transection. The patency of the vascular system was examined after a brief transcardial flush with heparinized saline followed by perfusion of red vinyl latex (N=12) or black indian ink (N=2). After various post-lesion survival times, five animals with intracranial optic nerve transection, four with intraorbital optic nerve transection, and five unoperated controls were perfused. Immediately, the vasculature was documented photographically as the optic nerve and orbital contents were carefully dissected.

Retinal wholemount preparation

The retinas of 16 mice were prepared as flat mounts. At the end of a 7-9 month postoperative survival time, animals were anesthetized with Avertin (0.03 ml/g body wt) and perfused transcardially with 20 ml 0.9% saline immediately followed by 100 ml of 20% formalin (commercial 38% formalin diluted 1:5 in saline) at 5 ml per minute. A shallow superior orienting cut was made from ora serrata to the middle of the cornea and the eyes were then dissected out in saline. Both transected and non-transected side retinas were prepared as wholemounts (Fig. 1) similar to the method of Stone ('66). Wholemounts were immersed

in a solution of 95% ethanol/4% formalin and pressed vitreal side up onto gelatin-coated slides by the use of Teflon tape and three 10-g brass weights for 30 minutes. The slides were transfered into 97% ethanol/3% glacial acetic acid for 30 min and then stained with 0.3% cresyl violet V (Schmid & Co., Stuttgart) for 1 min at 57'C. Following dehydration for 1 min in 95% ethanol and 3 min in absolute ethanol, the slide was cleared in Terpineol for 30 minutes. The retinas were then washed in Xylene for 2 min with agitation, coverslipped with Permount, and pressed under two 10-g weights for 24 hours. Both retinas, ipsilateral transection and contralateral control were mounted on the same slide and thus processed identically.

Data collection and ganglion cell analysis

All data collection and analysis were performed within the departmental Image Graphics Laboratory using a VAX 11/780 computer (Digital Equipment Corp, Maynard, MA) interfaced with an interactive, realtime Megatek Corp (San Diego, CA) 7210 graphics display system, and a Zeiss (New York, NY) microscope with automatic three axis motor-driven stage. Cells within a wholemounted retina were traced on an interactive data tablet using a camera lucida arrangement which allows simultaneous viewing of the user generated Megatek outline image over the microscope field.

Without the correct microscope filters, the metachromatic cells of the ganglion cell layer have a density and color

approximately equal to each other. The difference between darkly blue-staining glial cells and pink ganglion cells was maximized using 3 filters: Orange 81C, dydinium-doped glass, and blue 82A (Bessler Co). Since ganglion cells range widely in size, their identification was further based on the presence of nissl substance, irregular cytoplasmic boundaries, a large pale, vesicular nucleus and darkly stained nucleoli (Fig. 2). Displaced amacrine cells were not always discounted as easily as glial and endothelial cells.

After calibrating the microscope, data tablet, and graphics display, the wholemount perimeter outline was traced at 20x magnification. While still at low power, each wholemount quadrant was divided into inner, middle, and outer zones. Zone bondaries were established as 1/3 and 2/3 of the radial distance from the optic nerve head to the wholemount outer border. Retinal ganglion cell size and location was tabulated at 1600x from each group (control, intraorbital transection, intracranial transection + /- graft) according to the quadrant (superior, inferior, nasal, temporal) and zone. All cells meeting the above criteria were entered from a given high magnification field which was represented as one square within the overlayed sampling grid (Fig.s 3 & 4). Grid squares within a zone were selected at randomn by the computer and digitized until approximately a 2% sample was quantified. Cells whose center of mass was outside the square bondaries were rejected automatically after being digitized. A schematic display of cells traced as well as their

number minimized counting errors. Occasional slight sample field adjustments were required at retinal edges and large blood vessels. Since quantitative data on cell numbers and sizes are highly variable, nonparametric Kolnogorov-Smirnov could not be used. Thus, the SAS statistical package (SAS Institute Inc, Cary, NC) was run to analyze and compare retinal cell densities and frequency-cell area class histograms.

Electron microscopy

Optic nerve ultrastructure of eight mice was examined after standard processing for electron microscopy. Two groups of four animals each were sacrificed at 1 month and 3 months following intracranial transection alone. At the time of initial surgery each group had two adults and two neonates(P8-10).

RESULTS

Blood supply

In the rat and mouse the ophthalmic artery arises from the palatine branch of the pterygopalatine artery (Janes and Bounds,'55; Bugge,'70; Anderson,'70). From here, the murine ophthalmic artery runs along the lateral border of the trigeminal nerve's first division in the alisphenoid canal, enters the orbit through the anterior lacerated foramen and gives rise to the central retinal, ciliary, and corneoscleral arteries intraorbitally just proximal to the globe. Thus, the course of the main retinal blood supply is well separated from the optic nerve intracranially. In other animals, however, particularly higher primates, the ophthalmic artery and its central retinal branch run intracranially along the optic nerve as a branch of the internal carotid artery.

Using the intracranial surgical approach described above, the optic nerve was transected midway from foramen to chiasm thereby maintaining a patent blood supply to the retinal ganglion cells. In contrast, inadvertent intraorbital optic nerve transection disrupts blood supply to the retina, choroid, sclera, and ciliary body. With a different, recently developed, intraorbital transection technique (not described here) requiring careful extraction and isolation of the proximally penetrating central retinal artery, blood supply may be preserved. The

vascular supply to the nerve and eye was outlined by transcardial red vinyl latex perfusion in an unoperated control, intracranial and intraorbital optic nerve transection groups. After hardening, the latex maintains the vasculature in anatomic position for dissection and photography. In figures 5-7 the blood supply is illustrated for various survival times and surgical groups. In all five animals examined following intracranial optic nerve transections after one to nine month survivals, the vasculature was readily followed and patent to all eye components. Indian ink perfusion in two animals further confirmed the results. Thus, complete optic nerve transection of all components; vascular, neuronal and glial within its perineurial sheath; maintains retinal blood supply when performed intracranially, yet interrupts it when done intraorbitally.

Retinal ganglion cell analysis

The pattern of stained neurons over the retinal wholemount ganglion cell layer appears to be arranged in densely packed rays extending out from the optic nerve head, as best demonstrated in a control retina at mid power magnification. This well organized radial arrangement, in parallel with ganglion cell axons and central retinal artery main trunks, becomes increasingly disturbed in going from control to intracranially transected alone (Fig. 8), with complete deterioration seen in the intraorbitally sectioned mice. The individual ganglion cells themselves were of normal morphology in both transected and

grafted animals with no signs of chromatolysis.

Ganglion cells were not labelled or assigned to the three various classes; W, X, and Y; as described earlier (Stone and Fukuda,'74; Rowe and Stone,'76). On reviewing frequency by cell area class histograms as in Figures 9-17, clear trimodal distributions are not evident to define three distinct area classes. Thus, hypotheses on a particular cell classes' viability and regenerative capacity following optic nerve manipulation are not made.

Since retinal cell areas and densities are not normally distributed, nonparametric and parametric statistics were run. Parametric tests comparing transected, grafted, and control animals in cell density overall, by zone, and by 10 square micron area classes were run using the Waller-Duncan K-ratio T test (minimizes the Bayes risk under additive loss), the Duncan's Multiple range test (controls type I comparisonwise error rate), and the Student-Newman-Keuls test (controls type I experimentwise error rate under the complete null hypothesis). In Table 1, the values for cell density (# cells/sq. micron) and mean cell area (sq. microns) are presented. For each retina within a group, data is tabulated by zone (inner, middle, outer) and overall. The overall values required a weighted averaging of densities and mean areas by zone size.

The mean overall (combined inner, middle, and outer zone) cell density for transected, grafted, and control groups was 0.20812, 0.25799, and 0.44225 cells/sq. micron respectively

(Table 2). Statistical tests showed that these density differences were significant at the 0.05 level for both experimental versus control animals. Although grafted animal overall mean cell density was higher than that of transection alone, this difference was not significant at the K ratio 100 level.

In examining collected data by zone, control and grafted cell density both decrease with increasing distance from the optic nerve head. Controls changed from 0.49237 inner, 0.47730 mid, to 0.38976 cells/sq. micron outer, while grafts decreased from 0.31304, to 0.26674, to 0.22432 cells/sq. micron. The largest percentage change in cell density when comparing inner to outer zone values occurred in the grafted animals (Fig. 18) where the decrease was 28%. Interestingly, the mean cell density by zone was low and nearly constant across retinas having received optic nerve transection alone. This cell density change by zone is illustrated in Figures 19-21. Analysis of variance using the General Linear Models procedure was done. In cell areas 21-30 sq. microns the control inner cell density was significantly different($P<0.01$) from transected inner density, but not from grafted (Table 3) by all tests. Control retina middle zone was significantly different from both transection mid and grafted mid at this cell size. In the 31-40 sq. micron class, control inner was significantly different from both transected and grafted ($P=0.0006$) which was again true for control mid versus grafted and transection middle zones. The next four 10 sq. micron size

classes also each had controls significantly (P<0.001) different from both experimentals.

Nonparametric comparisons using Wilcoxon 2-sample, Kruskal-Wallis, and Median 2-sample tests to compare inner retinal densities between transection and grafted animals also indicate significant differences. The probability values for the significant difference of inner density means (Table 4) using these tests were all less than 0.05. With a parametric comparison, the T-test also supports a significant (P<0.05) difference between transection and grafted inner zone cell density. There is thus an indication that a sciatic and neonatal optic nerve intracranial graft may be promoting survival of neurons whose bodies lie within the inner retina.

Unlike cell density, overall mean cell area in control and experimental groups was not significantly different. As shown in Figures 9-11, the control animal cell histogram shapes and mean areas were very similar to other studies (Grafstein and Ingoglia,'82; Allcutt et al.,'84a). As mentioned, control cell sizes are not normally distributed but rather are skewed to larger size classes from a modal area lying between 21 and 30 sq. microns in the inner, mid, and outer retina. The grafted animals also had a constant cell size mode across retinal zones, yet it was in the 11-20 sq. micron cell class, thus smaller than that of controls. Transected animal cell mode however increased from 11-20 to 21-30 sq. microns in going from inner to middle or outer retina.

Following transection alone or grafting the mean percentage of cells in the modal class area increased. In controls 24.9 % of the cells were in the mode while this increased to 31.7% in transected, and 34.0% in grafted animals. Experimental retinas had a smaller proportion of cells in the larger cell area classes.

The overall mean cell area decreased from control 36.98, transected 29.30, to grafted 27.00 sq. microns. Mean cell area by zone decreased from inner to outer retinal zones in controls (8.6%) and transected animals (16.7%) whereas grafted mean cell area was nearly constant at 27 sq. microns, rising only slightly in the middle zone. Comparing zones between retinal groups, there is a 17% reduction from control in transected inner mean cell area and 30% in grafted animals. Within the middle zone the decrease from control was 20% in transected and 26% in grafted mice. The change in outer retinal mean cell area for both transected and graft was 24%.

Coupled with the above finding of significantly increased cell density in the grafted inner retina, there appears to be an increase in the number of small cells surviving in grafted versus transection thus decreasing the overall mean calculated and shifting the mode.

Electron microscopy

The optic nerves of adult mice were examined with the electron microscope one month (N=4) or three months (N=4)

following intracranial transection alone. Upon nerve dissection the region of previous experimental transection, although now continuous, could be identified by its decreased caliber and yellowed color. Skip serial sectioning was done on a 3-4 mm optic nerve segment removed en bloc to include transection site with proximal and distal segments. Several thin sections (electron microscopy) and one micron sections (light microscopy) were cut followed by skipping 100 one-micron sections throughout the full nerve piece. By this method, the axonal reaction distal and proximal to the transection was reviewed comprehensively.

At one month following transection alone in an adult mouse, Figure 22 shows many axons in the proximal nerve stump. Some axons are clearly degenerating, yet in another group the myelin sheath and axoplasm appear normal. Electron micrographs of an optic nerve 3 months following transection still show some normal looking axons in the stump proximal to the transection (Fig. 23) with appearance of remyelination.

Since sections closer to the eye had qualitatively more myelinated axons than sections more distal in the proximal stump, a process of remyelination may be proceeding along an eye-to-diencephalon gradient. Similarly, myelination in the early postnatal rat develops in this direction (Skoff et al.,'80). Others have suggested that functional recovery and survival may be determined by the success of this remyelination after injury (Clifford-Jones et al.,'80; Wender et al.,'81).

In this group receiving transection alone without grafting,

there were many proximal nerve segments with both myelinated and unmyelinated fibers extending up to, but not across the point of transection. Careful serial one micron and thin sections showed an absence of healthy axons in the distal nerve segment. The point of surgical transection appears to present a barrier to further rectilinear growth if not abutted by a nerve graft. In Figure 24, the fibers seem to be changing course and thus running longitudinally in this axially cut section. There is clear evidence that the necessary prerequisites for regeneration are present with ganglion cell survival and axonal viability up to the lesion. Elongation and increased cell survival may be promoted through the improved microenvironment presented by implants in the grafted animal group.

DISCUSSION

These experiments have examined the problems of CNS regeneration by both a qualitative and quantitative approach. Several important points have been demonstrated through using a well-defined rodent visual system as a model.

First, the intracranial surgical approach described and developed here for transection of the optic nerve clearly preserves blood supply to the retina and orbital contents. The difference between intraorbital and intracranial optic nerve transection is anatomically well demonstrated by intravascular latex injection shown in Figures 6 and 7. Inadvertent intraorbital transection, as used in earlier CNS regeneration studies in the rodent visual system, destroys blood supply. Thus, the second point found here that patency of the central retinal blood supply as it enters the back of the eye is a prerequisite for any ganglion cell survival and regeneration. In Figure 8, the change in cell size and density over the wholemount at nine months following intracranial optic nerve transection versus control is shown. Third, quantitative retinal ganglion cell wholemount analysis demonstrates significant and specific effects of an intracranial graft. The control group cell density and area data agree well with other mouse studies (Grafstein and Ingoglia,'82; Allcutt et al.,'84a). Finally, qualitative evidence of surviving myelinated and unmyelinated optic axons by electron

microscopy is presented (Figures 22-24) for animals receiving intracranial transections one and three months earlier.

In the report by Misantone et al. ('82) ganglion cell number in rat after intracranial crush was stable at one month with decreased cell RNA content. Yet, there was no quantitative data presented nor mention of the difference between crush and transection lesions. Vidal-Sanz et al. ('85) grafted sciatic nerve to optic nerve head but again exact cell numbers were not given. Grafstein and Ingoglia ('82) presented actual surviving cell numbers and areas for control versus intracranially transected over time. Each of the time points, however, had small N-values, either one or two mice. Their study did not attempt to examine the effects of an intracranial graft. Allcutt et al. ('84) looked at intraorbital crush in mice and reported that only 10% of cells survived at one month. Similarly to this report, he found a greater proportion of small cells survive. Yet, a crush injury, particularly intraorbitally, may not be comparable.

In the rat following intracranial optic nerve transection and grafting, Richardson et al. ('82) noted survival and regeneration of some axons. Sciatic nerve grafting was also attempted and was found not to enhance axonal survival. These investigators reported that retinal architecture was preserved with little ganglion cell loss, yet quantitive data was not presented.

As mentioned earlier in the introduction, others using the optic nerve and retina model in various animals have simply

described ganglion cell survival or axon numbers following section. However, this project attempted to increase cell survival and thus regeneration by further examining variables of axotomy distance, blood supply, and grafting. In reviewing the literature, it is noted here first that there appears to be greater ganglion cell survival with increasing distance from axotomy to cell body, yet there is decreasing regenerative axonal sprouting. Many experiments have confounded their model by using crush lesions which create unknown and unreliable neuronal/vascular changes or by sectioning in an environment not representative of central nervous system, such as the retina lacking oligodendrocytes.

Since projected total cell numbers and density values depend upon the assumption that the analysis perimeter size of a wholemounted retina equals the actual in vivo area of the globe, processing shrinkage could cause errors. Hughes ('75) observed for the cat that shrinkage was most marked around the periphery of the retina and along cuts or tears in the tissue. Once the retina was fixed to the gelatinized slide a minimal change in total retinal area was observed.

Axotomy induced shrinkage and redistribution of area class (ie. with shrinkage medium-sized neurons are now tabulated as increasing the small cell class population) may be another problem. The data may be further skewed toward smaller area values by the inevitable mistaken inclusion of glial cells as small neurons. However, Allcutt et al. ('84a) believe that within

retinas of lesioned animals the constancy of relative distributions with time suggests that a change in cell size distribution is due to varied cell death by size and not shrinkage. With any formalin fixation procedure an unknown amount of perikaryal shrinkage may effect absolute numbers in a set area class but not relative numbers between classes. Wassle et al. ('75) reported that individual cell bodies shrunk by 20-30% as a consequence of histological processing of wholemounts. The soma areas here were derived from stained, dehydrated, and mounted retinas and not corrected for shrinkage.

Clearly these experiments demonstrate the ability of small and intermediate cell area classes to survive transection of their axons intracranially. This is especially true when compared to intraorbital transections. After the addition of either sciatic or neonatal optic nerve grafts intracranially, the number of surviving cells within the retina is significantly increased. Further, the increased viability is in the small ganglion cell sizes as the mode of mean cell area has shifted down to the 21-30 sq. micron area class and increased the proportion of cells within it substantially.

Trophic influences provided by a graft may be retrogradely transported only limited axonal distances thus effecting cells closer to the optic nerve head preferentially. Also consistent with these results is the theory of programed cell death which would not be aborted in outlying neurons by receiving trophic factors before a critical survival time point.

The data comparing overall cell density by group, as well as by size classes in transection vs. graft had consistent differences which were very close to being significant. Trends in this data are quite evident yet, due to the small N-values(5,4 & 7) within these groups, significant differences, particularly in multigroup analysis, could not be confirmed. In order to solve this problem an increased N with more animals would be necessary. Since these experiments would then require many resources with substantial manpower and time required for data collection, the added result would be costly.

It appears now that ganglion cell survival, and axonal sprouting with effective elongation are controlled by different factors. These results, however, have demonstrated that axonal transection (while maintaining blood supply) is not a lethal event and that cell survival is significantly increased in specific ways with peripheral and neonatal nerve grafts. The first step prerequisite to any mammalian CNS regeneration must be survival of the parent cell body. Factors maximizing this would be necessary for optimal promotion of axonal elongation and ultimately, functional regeneration.

LIST OF FIGURES

1. Control retinal wholemount overview (40x) with high power inset.

2. Control retina, middle zone (504x), identification of neurons in the ganglion cell layer.

3. Wholemount perimeter and zone boundaries with actual 2% sampling areas used in RE17, intracranially grafted animal.

4. Wholemount perimeter and zone boundaries with actual sampled cell areas, comparing 6% to 2% sample size.

5. Unoperated control mouse blood supply.

6. Intracranial optic nerve transection blood supply after 9 month survival.

7. Intraorbital optic nerve transection blood supply after 10 day survival.

8. Photomicrograph of cell size and density after 9 month survival; intracranial optic nerve transection v. contralat. control.

18. Graph of cell density by zone comparing groups.

19. Control mouse; inner, middle, and outer fields.

20. Transection alone mouse; inner, middle, and outer fields.

21. Grafted mouse; inner, middle, and outer fields.

22. Electron micrograph, proximal nerve stump, 1 month following intracranial transection alone.

23. Electron micrograph, proximal nerve stump, 3 months following intracranial transection alone.

24. Electron micrograph, site of transection, 3 months following intracranial transection alone.

Figures 1, 5-7,and 22-24 are used with permission from this author's paper with Madison and Sidman.

FIGURE 1:

Control retinal wholemount. This retina was prepared from the contralateral side of a mouse receiving optic nerve transection alone nine months earlier. Since both retinas were mounted on one slide, processing of control and transection wholemounts was identical.

A) Low power (40x) overview of wholemount showing radial cuts made to allow retina to lie flat. Choroid and pigmented epithelium are stripped away and the central retinal artery paths can be seen at low power as tracks void of darkly staining cells.

B) Higher power field from the outlined inset in the above. Finer branches of arteries are seen however, cell digitization was done at even higher magnification. Size bar = 20 micron.
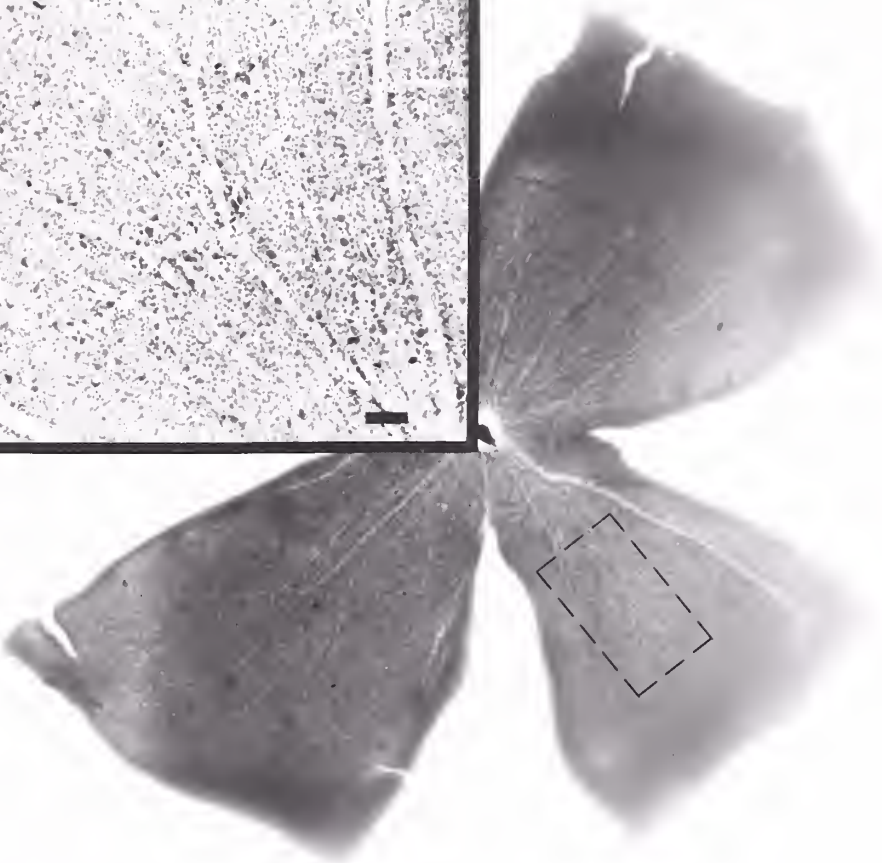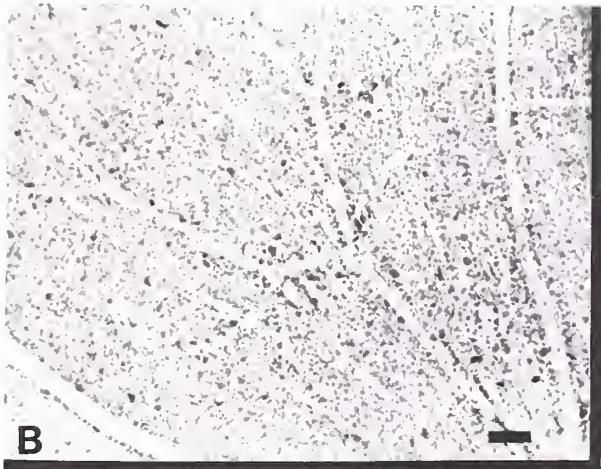
FIGURE 2:

Photomicrograph of cells in the retinal ganglion cell layer at 504x magnification. Since cells within this frame are not all in the same focal plane, fine focusing was varied to best visualize cell outlines when digitizing their perimeters. Note the different sizes of ganglion cells(g) with their nissl substance(ns), large pale nucleus(nu), and dark nucleoli(n).
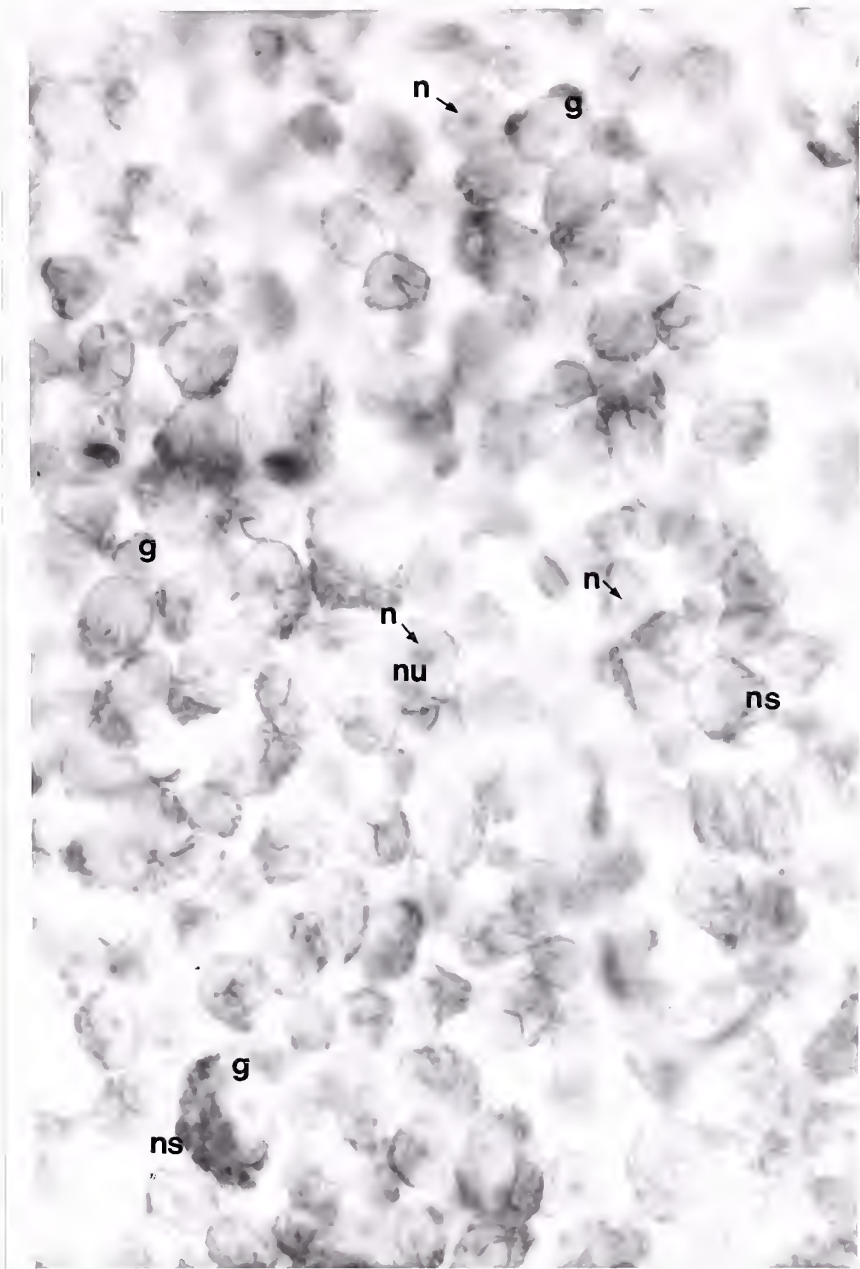
FIGURE 3:

Computer drawn plot of retinal wholemount analysis perimeter. Each retinal leaf was separated into 3 zones; inner, middle, and outer; established as 1/3 and 2/3 of the radial distance from the optic nerve head to the outer edge. Due to the large central retinal artery trunks, the optic cup, and the high axon density at the optic nerve head (physiologic blind spot) few neurons are present here. Thus, the inner zone does not include this small area in analysis. Each marked "+" represents an area of cell digitization making up a 2% sample size in this animal grafted intracranially nine months earlier. Calibration bar = 1 mm.
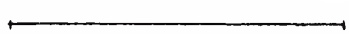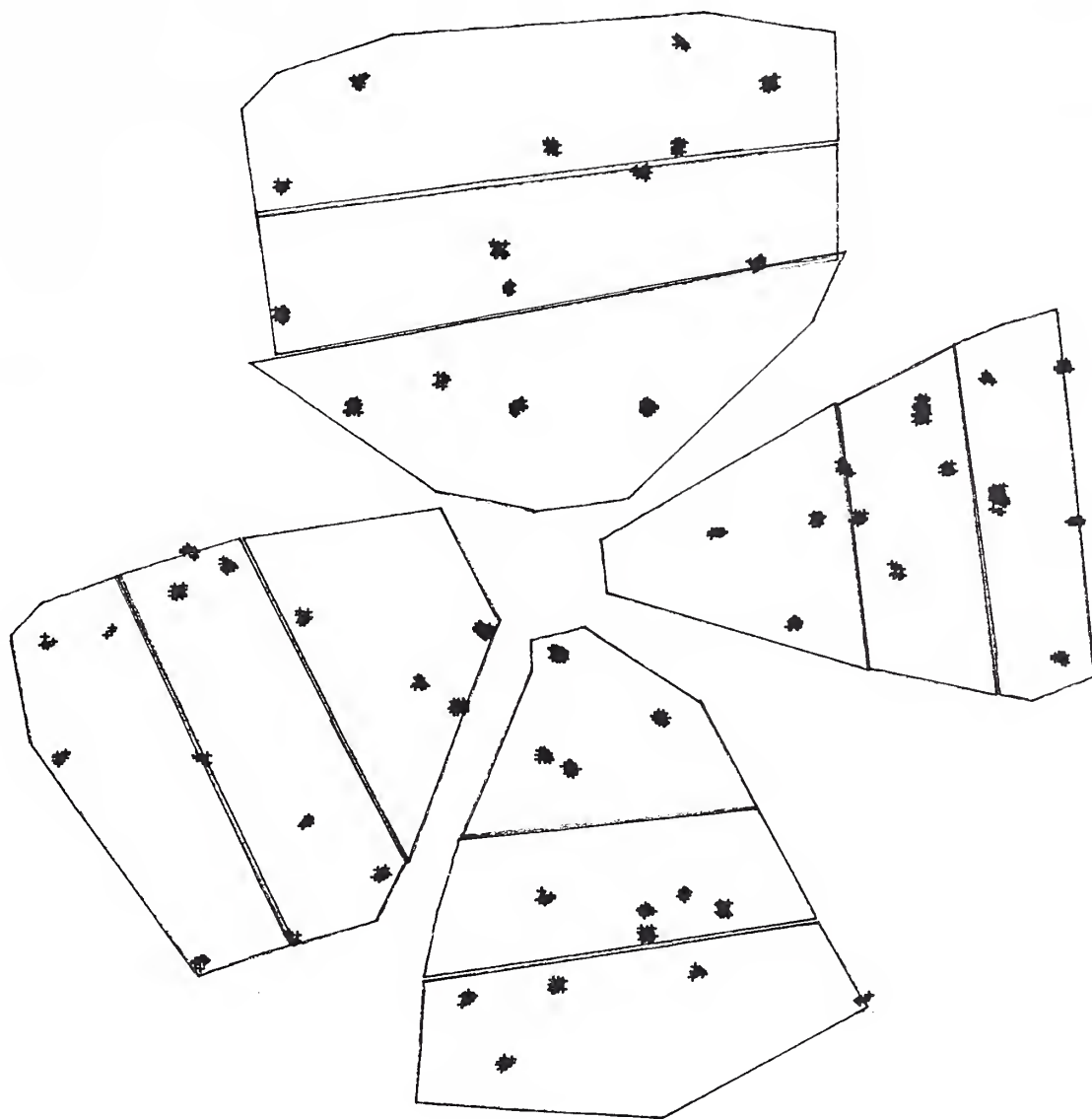
LEN= 0.1E+04 SCALE=0.872220E+00

RE17   1- 4, 1 ZLEV= 1.00 VIEW ANG=   0.00   0.00

FIGURE 4:

Computer drawn plot of retinal wholemount analysis perimeter comparing 6% to 2% sampling grid. Frequency analysis run on two sampling levels reveals that 2% sampling is sufficient and accurately represents the whole population of a zone. All data was therefore collected and analyzed at this later sampling level. Calibration bar = 1 mm.
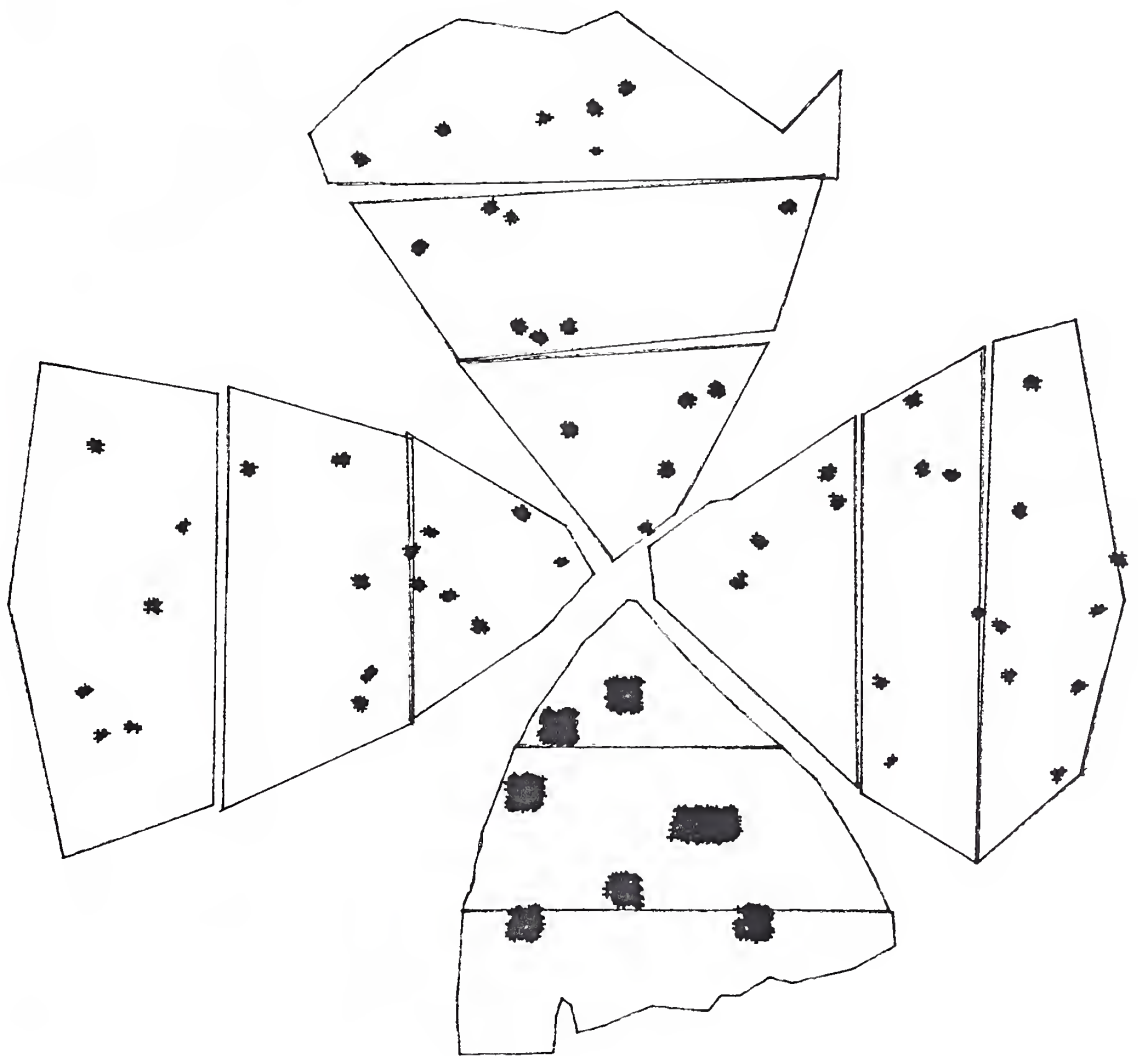
LEN= 0.1E+0+ SCALE=0.672878E+00

RET1   1- 4. 1 +ZLEV= 1.00 VIEW ANG=   0.00   0.00

FIGURE 5:

Unoperated control mouse blood supply. Photographs taken through operating microscope, dorsal view of control mouse injected with red vinyl latex (mouse anterior is at the top, posterior at the bottom).

A)   The frontal pole of the brain has been removed to the optic chiasm. The eyes are visible as large black masses on either side of the head. Anterior cerebral arteries are filled with red latex (a). Solid arrow indicates intracranial portion of optic nerve where transection would occur. Open arrow head indicates palatine artery on the lateral border of the trigeminal nerve(5x).

B)   The ophthalmic artery is shown by double arrowhead. The palatine portion of the pterygopalatine artery enters the orbit through the anterior lacerated foramen with the trigeminal nerve and branches into the ophthalmic(superior and inferior) and posterior superior alveolar arteries(7.5x).

C)   The posterior superior alveolar artery leaves the orbital fossa(open arrow). The palatine artery(open arrowhead) and entrance of the ophthalmic artery(double arrowhead) into the back of the eye are shown. Orbital portion of optic nerve is seen as a solid arrow(12x).

D)   The eye is opened and removing the lens with vitreous allows visualization of the latex filled retinal arteries, thus demonstrating patent blood supply to the ganglion cell layer (12x).
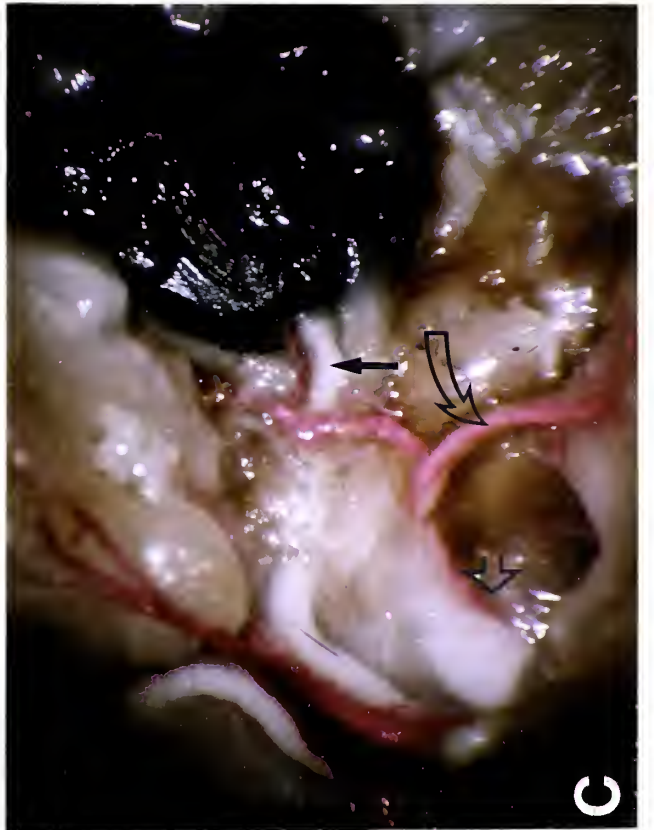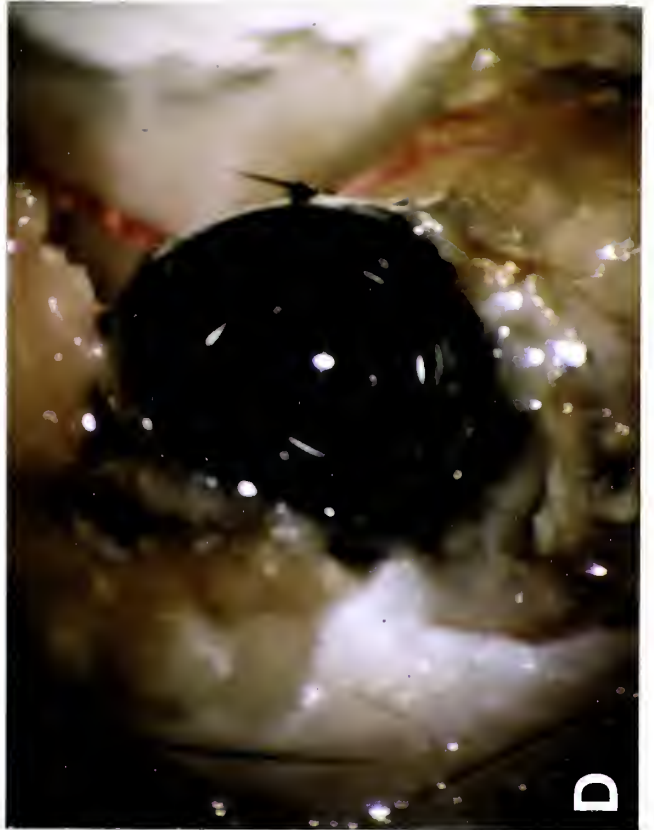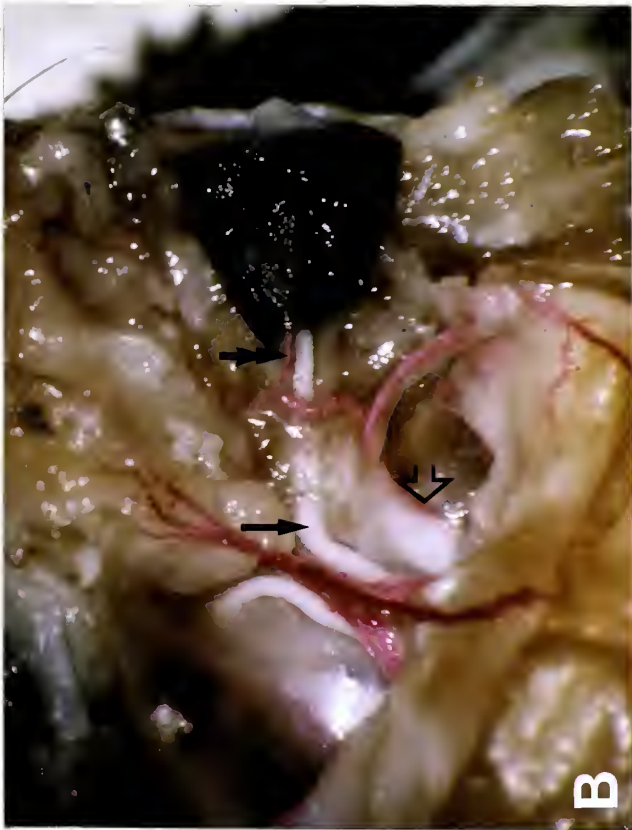
FIGURE 6:

Intracranial optic nerve transection alone blood supply. Photographs taken and oriented identically to above in an animal receiving intracranial transection alone nine months earlier.

A) As in control figure, anterior cerebral arteries are filled with red latex(a). Intracranial optic nerve transection site (open arrow) is shown (5x).

B) Increased magnification of transection site(open arrow). A cable of gelatinous material is filling the transection site. The internal carotid and anterior cerebral arteries are seen with many new arterial twigs representing revascualrization (12x).

C) Dorsal aspect of the orbit has been removed and a patent blood supply is maintained. The ophthalmic(double arrowhead) and anterior cerebral(a) arteries are noted. Suture needles indicate a short segment of superior alveolar artery that was incompletely filled with latex. The intraorbital portion of optic nerve is noted by a curved arrow (12x).

D) The eye is opened, lens and vitreous material removed to show retinal arteries are still being filled nine months after intracranial transection (12x).

FIGURE 7:

Intraorbital optic nerve transection blood supply. Surgical approach for intraorbital optic nerve transection 10 days earlier has largely allowed survival of patent blood supply to other orbital components, yet not the retina.

A) Blood supply to lacrimal gland and other dorsal orbital contents. Anterior cerebral artery(a) is filled with latex (12x).

B) The lacrimal gland has been removed to expose the contents of the orbit. Both the intracranial portion of optic nerve(solid arrow) and site of intraorbital optic nerve transection (double arrowhead) are shown. Red vinyl latex fills the posterior superior alveolar and ophthalmic arteries to the point of transection (7.5x).

C) Higher magnification view of above. The posterior superior alveolar artery is reflected dorsally and medially(open arrow) to expose the branch point of the ophthalmic artery. The double arrowheads indicate the position where the transected ophthalmic artery would have entered the back of the eye with the optic nerve. Proximal and distal stumps are shown with two small curved arrows (12x).

D) The eye is opened as before and lens with vitreous removed. There is no red latex visible to indicate a surviving ganglion cell layer blood supply. The eye cup is enveloped with collagenous scar tissue and markedly shrunken overall (12x).
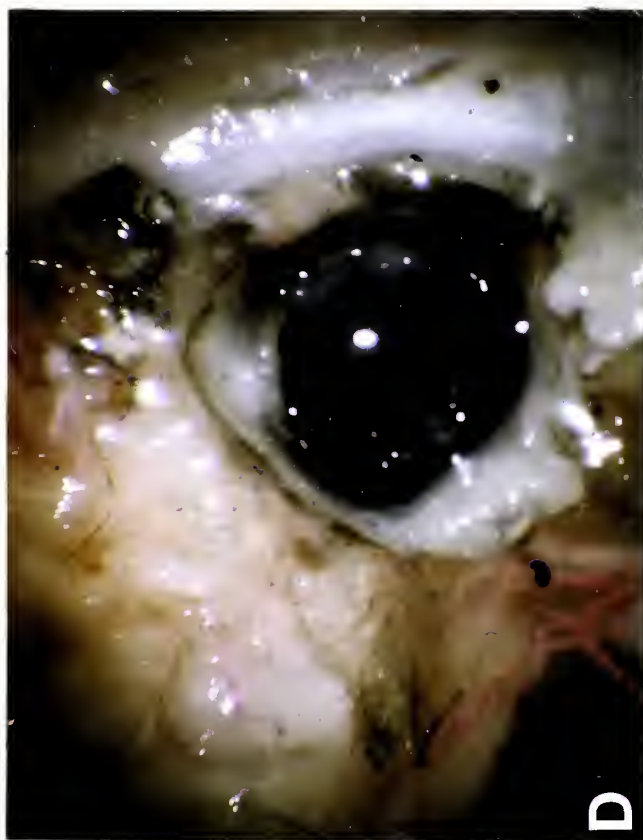
FIGURE 8:

Mid magnification micrographs comparing cell size and density in the retinal ganglion cell layer, intracranial transection versus contralateral control.

A) Retina ipsilateral to intracranial transection alone performed nine months earlier. Calibration bar = 10 microns.

B) Contralateral control wholemount to above, both mounted and processed together on the same slide. Note the densely packed radial organization of cell bodies separated by blood vessels. Calibration bar = 10 microns.

FIGURE 9:

Histogram, inner zone of control retina. Cell frequency by 10 sq. micron area classes is plotted for a representative control wholemount, RE18. Cumulative frequency, percent, and cumulative percent are given. The two following figures are the middle and outer zones of this same retina for verticle comparison.

FREQUENCY BAR CHART

MIDPOINT AREA	FREQ	CUM. FREQ	PERCENT	CUM. PERCENT
5	5	5	0.80	0.80
15	81	86	12.98	13.78
25	125	211	20.03	33.81
35	144	355	23.08	56.89
45	110	465	17.63	74.52
55	67	532	10.74	85.26
65	43	575	6.89	92.15
75	26	601	4.17	96.31
85	7	608	1.12	97.44
95	6	614	0.96	98.40
105	2	616	0.32	98.72
115	3	619	0.48	99.20
125	3	622	0.48	99.68
135	2	624	0.32	100.00
145	0	624	0.00	100.00
155	0	624	0.00	100.00
165	0	624	0.00	100.00
175	0	624	0.00	100.00
185	0	624	0.00	100.00
195	0	624	0.00	100.00

FREQUENCY

FIGURE 10:

Histogram, middle zone of control retina. Cell frequency by 10 sq. micron area class is plotted for this representative control wholemount, RE18 (same as previous Figure). Cumulative frequency, percent, and cumulative percent are given.

FREQUENCY BAR CHART

MIDPOINT AREA	FREQ	CUM. FREQ	PERCENT	CUM. PERCENT
5	2	2	0.22	0.22
15	113	115	12.24	12.46
25	220	335	23.84	36.29
35	179	514	19.39	55.69
45	150	664	16.25	71.94
55	103	767	11.16	83.10
65	56	823	6.07	89.17
75	34	857	3.68	92.85
85	24	881	2.60	95.45
95	15	896	1.63	97.07
105	15	911	1.63	98.70
115	5	916	0.54	99.24
125	2	918	0.22	99.46
135	3	921	0.33	99.78
145	1	922	0.11	99.89
155	1	923	0.11	100.00
165	0	923	0.00	100.00
175	0	923	0.00	100.00
185	0	923	0.00	100.00
195	0	923	0.00	100.00

FREQUENCY

10 20 30 40 50 60 70 80 90 100 110 120 130 140 150 160 170 180 190 200 210 220

FIGURE 11:

Histogram, outer zone of control retina. Cell frequency by 10 sq. micron area classes is plotted for this representative control wholemount, RE18 (as p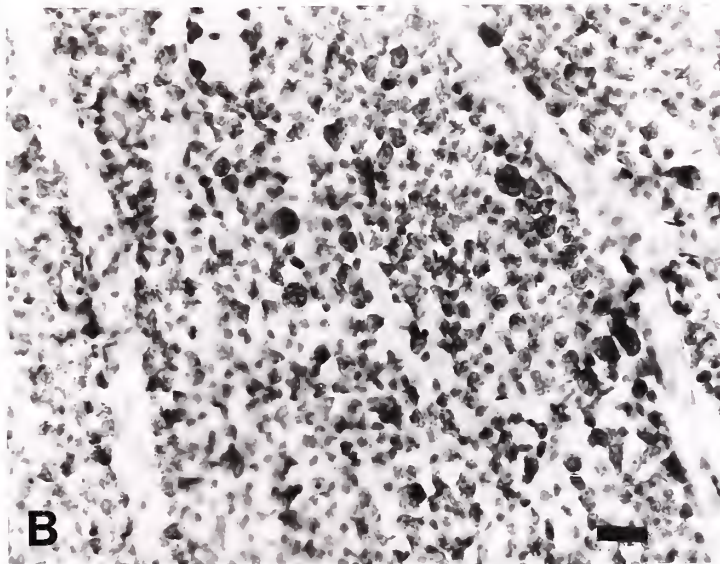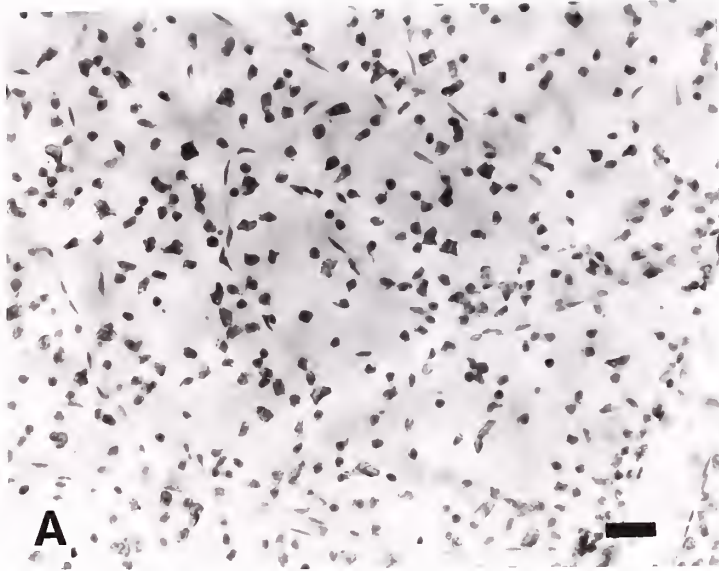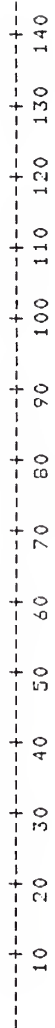revious two figures). Cumulative frequency, percent, and cumulative percent are given. Verticle comparison should be made with the previous two figures.

FREQUENCY BAR CHART

MIDPOINT AREA	FREQ	CUM. FREQ	PERCENT	CUM. PERCENT
5	3	3	0.64	0.64
15	94	97	20.17	20.82
25	129	226	27.68	48.50
35	70	296	15.02	63.52
45	55	351	11.80	75.32
55	43	394	9.23	84.55
65	28	422	6.01	90.56
75	12	434	2.58	93.13
85	13	447	2.79	95.92
95	7	454	1.50	97.42
105	5	459	1.07	98.50
115	3	462	0.64	99.14
125	1	463	0.21	99.36
135	1	464	0.21	99.57
145	0	464	0.00	99.57
155	1	465	0.21	99.79
165	1	466	0.21	100.00
175	0	466	0.00	100.00
185	0	466	0.00	100.00
195	0	466	0.00	100.00

```
MIDPOINT
AREA

  5  |**
     |
 15  |*********************
     |
 25  |****************************
     |
 35  |***************
     |
 45  |************
     |
 55  |**********
     |
 65  |******
     |
 75  |***
     |
 85  |***
     |
 95  |****
     |
105  |***
     |
115  |**
     |
125  |*
     |
135  |*
     |
145  |
     |
155  |*
     |
165  |*
     |
175  |
     |
185  |
     |
195  |
     |
     ----+----+----+----+----+----+----+----+----+----+----+----+----+
        10   20   30   40   50   60   70   80   90  100  110  120  130
                                FREQUENCY
```

FIGURE 12:

Histogram, inner zone of transection alone retina. Cell frequency by 10 sq. micron area class is plotted for a representative transection wholemount, RE14. Cumulative frequency, percent, and cumulative percent are given. The two following figures are the middle and outer zones of this same retina for verticle comparison.

FREQUENCY BAR CHART

MIDPOINT AREA	FREQ	CUM. FREQ	PERCENT	CUM. PERCENT
5	11	11	4.49	4.49
15	130	141	53.06	57.55
25	55	196	22.45	80.00
35	28	224	11.43	91.43
45	16	240	6.53	97.96
55	3	243	1.22	99.18
65	1	244	0.41	99.59
75	1	245	0.41	100.00
85	0	245	0.00	100.00
95	0	245	0.00	100.00
105	0	245	0.00	100.00
115	0	245	0.00	100.00
125	0	245	0.00	100.00
135	0	245	0.00	100.00
145	0	245	0.00	100.00
155	0	245	0.00	100.00
165	0	245	0.00	100.00
175	0	245	0.00	100.00
185	0	245	0.00	100.00
195	0	245	0.00	100.00

Bar chart (FREQUENCY axis: 10 20 30 40 50 60 70 80 90 100 110 120 130):

```
  5 |*******
 15 |**********************************************************************************************************************************
 25 |*******************************************************
 35 |****************************
 45 |****************
 55 |***
 65 |*
 75 |*
 85 |
 95 |
105 |
115 |
125 |
135 |
145 |
155 |
165 |
175 |
185 |
195 |
    ----+----+----+----+----+----+----+----+----+----+----+----+----+
       10   20   30   40   50   60   70   80   90  100  110  120  130
                              FREQUENCY
```
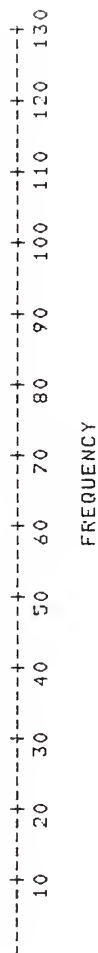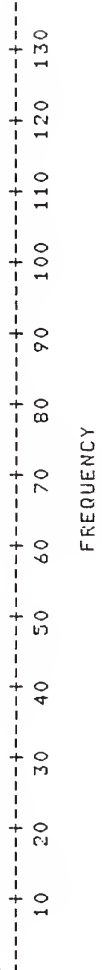
FIGURE 13:

Histogram, middle zone of transection alone retina. Cell frequency by 10 sq. micron size class is plotted for this representative transection alone wholemount, RE14 (as in the previous figure). Cumulative frequency, percent, and cumulative percent are given.

FREQUENCY BAR CHART

MIDPOINT AREA	FREQ	CUM. FREQ	PERCENT	CUM. PERCENT
5	7	7	2.72	2.72
15	136	143	52.92	55.64
25	72	215	28.02	83.66
35	23	238	8.95	92.61
45	11	249	4.28	96.89
55	4	253	1.56	98.44
65	2	255	0.78	99.22
75	2	257	0.78	100.00
85	0	257	0.00	100.00
95	0	257	0.00	100.00
105	0	257	0.00	100.00
115	0	257	0.00	100.00
125	0	257	0.00	100.00
135	0	257	0.00	100.00
145	0	257	0.00	100.00
155	0	257	0.00	100.00
165	0	257	0.00	100.00
175	0	257	0.00	100.00
185	0	257	0.00	100.00
195	0	257	0.00	100.00

```
MIDPOINT
AREA

   5  |****
  15  |*********************************************************************************
  25  |************************************
  35  |***********
  45  |******
  55  |**
  65  |*
  75  |*
  85  |
  95  |
 105  |
 115  |
 125  |
 135  |
 145  |
 155  |
 165  |
 175  |
 185  |
 195  |
      ---+----+----+----+----+----+----+----+----+----+----+----+----+----+
        10   20   30   40   50   60   70   80   90  100  110  120  130
                                FREQUENCY
```
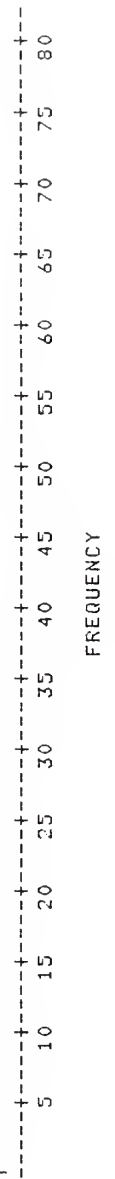
FIGURE 14:

Histogram, outer zone of transection alone retina. Cell frequency by 10 sq. micron area class is plotted for this representative transection alone retina, RE14 (as previous two figures). Cumulative frequency, percent, and cumulative percent are given. A verticle comparison within the group can be made with the two previous figures.

FREQUENCY BAR CHART

MIDPOINT AREA		FREQ	CUM. FREQ	PERCENT	CUM. PERCENT
5	**	2	2	1.08	1.08
15	***	62	84	44.32	45.41
25	***	59	143	31.89	77.30
35	**************************	27	170	14.59	91.89
45	********	8	178	4.32	96.22
55	****	4	182	2.16	98.38
65	**	2	184	1.08	99.46
75	*	1	185	0.54	100.00
85		0	185	0.00	100.00
95		0	185	0.00	100.00
105		0	185	0.00	100.00
115		0	185	0.00	100.00
125		0	185	0.00	100.00
135		0	185	0.00	100.00
145		0	185	0.00	100.00
155		0	185	0.00	100.00
165		0	185	0.00	100.00
175		0	185	0.00	100.00
185		0	185	0.00	100.00
195		0	185	0.00	100.00

```
----+----+----+----+----+----+----+----+----+----+----+----+----+----+----+----+
    5   10   15   20   25   30   35   40   45   50   55   60   65   70   75   80
```
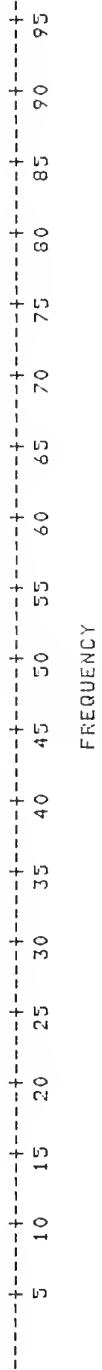
FREQUENCY

FIGURE 15:

Histogram, inner zone of grafted retina. Cell frequency by 10 sq. micron area class is plotted for a representative intracranially grafted animal, RET7. Cumulative frequency, percent, and cumulative percent are given. The two following figures are the middle and outer zones of this same retina for verticle comparison.

FREQUENCY BAR CHART

MIDPOINT AREA		FREQ	CUM. FREQ	PERCENT	CUM. PERCENT
5	*********	9	9	3.57	3.57
15	***	96	105	38.10	41.67
25	**************************************	75	180	29.76	71.43
35	*******************	38	218	15.08	86.51
45	*********	18	236	7.14	93.65
55	******	12	248	4.76	98.41
65	***	3	251	1.19	99.60
75	*	1	252	0.40	100.00
85		0	252	0.00	100.00
95		0	252	0.00	100.00
105		0	252	0.00	100.00
115		0	252	0.00	100.00
125		0	252	0.00	100.00
135		0	252	0.00	100.00
145		0	252	0.00	100.00
155		0	252	0.00	100.00
165		0	252	0.00	100.00
175		0	252	0.00	100.00
185		0	252	0.00	100.00
195		0	252	0.00	100.00

```
----+----+----+----+----+----+----+----+----+----+----+----+----+----+----+----+----+----+----+
    5   10   15   20   25   30   35   40   45   50   55   60   65   70   75   80   85   90   95
                                              FREQUENCY
```
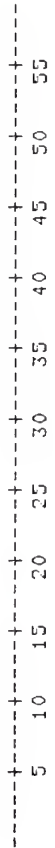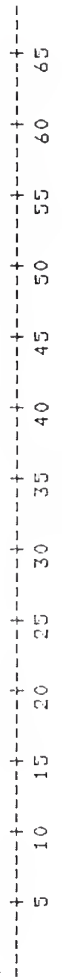
FIGURE 16:

Histogram, middle zone of grafted retina. Cell frequency by 10 sq. micron area class is plotted for this representative intracranially grafted wholemount, RET7 (as the previous figure). Cumulative frequency, percent, and cumulative percent are given.

FREQUENCY BAR CHART

MIDPOINT AREA		FREQ	CUM. FREQ	PERCENT	CUM. PERCENT
5	|*************	13	13	5.96	5.96
15	|***	59	72	27.06	33.03
25	|***	59	131	27.06	60.09
35	|**************************************	38	169	17.43	77.52
45	|************************	24	193	11.01	88.53
55	|***************	15	208	6.88	95.41
65	|*****	5	213	2.29	97.71
75	|****	4	217	1.83	99.54
85	|	0	217	0.00	99.54
95	|*	1	218	0.46	100.00
105	|	0	218	0.00	100.00
115	|	0	218	0.00	100.00
125	|	0	218	0.00	100.00
135	|	0	218	0.00	100.00
145	|	0	218	0.00	100.00
155	|	0	218	0.00	100.00
165	|	0	218	0.00	100.00
175	|	0	218	0.00	100.00
185	|	0	218	0.00	100.00
195	|	0	218	0.00	100.00

```
----+----+----+----+----+----+----+----+----+----+----+----+
    5   10   15   20   25   30   35   40   45   50   55
                         FREQUENCY
```

FIGURE 17:

Histogram, outer zone of grafted retina. Cell frequency by 10 sq. micron area class is plotted for this representative intracranially grafted wholemount, RET7 (as the two previous figures for verticle comparison). Cumulative frequency, percent, and cumulative percent are given. Horizontal comparisons across groups should be noted in inner(Fig.s 9, 12, 15), middle (Fig.s 10, 13, 16), and outer(Fig.s 11, 14, 17) zones.

FREQUENCY BAR CHART

MIDPOINT AREA		FREQ	CUM. FREQ	PERCENT	CUM. PERCENT
5	******	5	5	2.67	2.67
15	**	68	73	36.36	39.04
25	************************************	48	121	25.67	64.71
35	********************	26	147	13.90	78.61
45	****************	20	167	10.70	89.30
55	*******	8	175	4.28	93.58
65	******	7	182	3.74	97.33
75	**	2	184	1.07	98.40
85		0	184	0.00	98.40
95	**	2	186	1.07	99.47
105		0	186	0.00	99.47
115	*	1	187	0.53	100.00
125		0	187	0.00	100.00
135		0	187	0.00	100.00
145		0	187	0.00	100.00
155		0	187	0.00	100.00
165		0	187	0.00	100.00
175		0	187	0.00	100.00
185		0	187	0.00	100.00
195		0	187	0.00	100.00

```
    ----+----+----+----+----+----+----+----+----+----+----+----+----+
        5   10   15   20   25   30   35   40   45   50   55   60   65
                                  FREQUENCY
```

FIGURE 18:

Graph of cell density by zone from data in Table 2. In moving from optic nerve head to outer retina cell density decreases 21% in control, and 28% in grafted animals. Note however, mean cell density of transected animals is low and nearly constant across the retina. This is illustrated in micrographs (Figures 19-21).
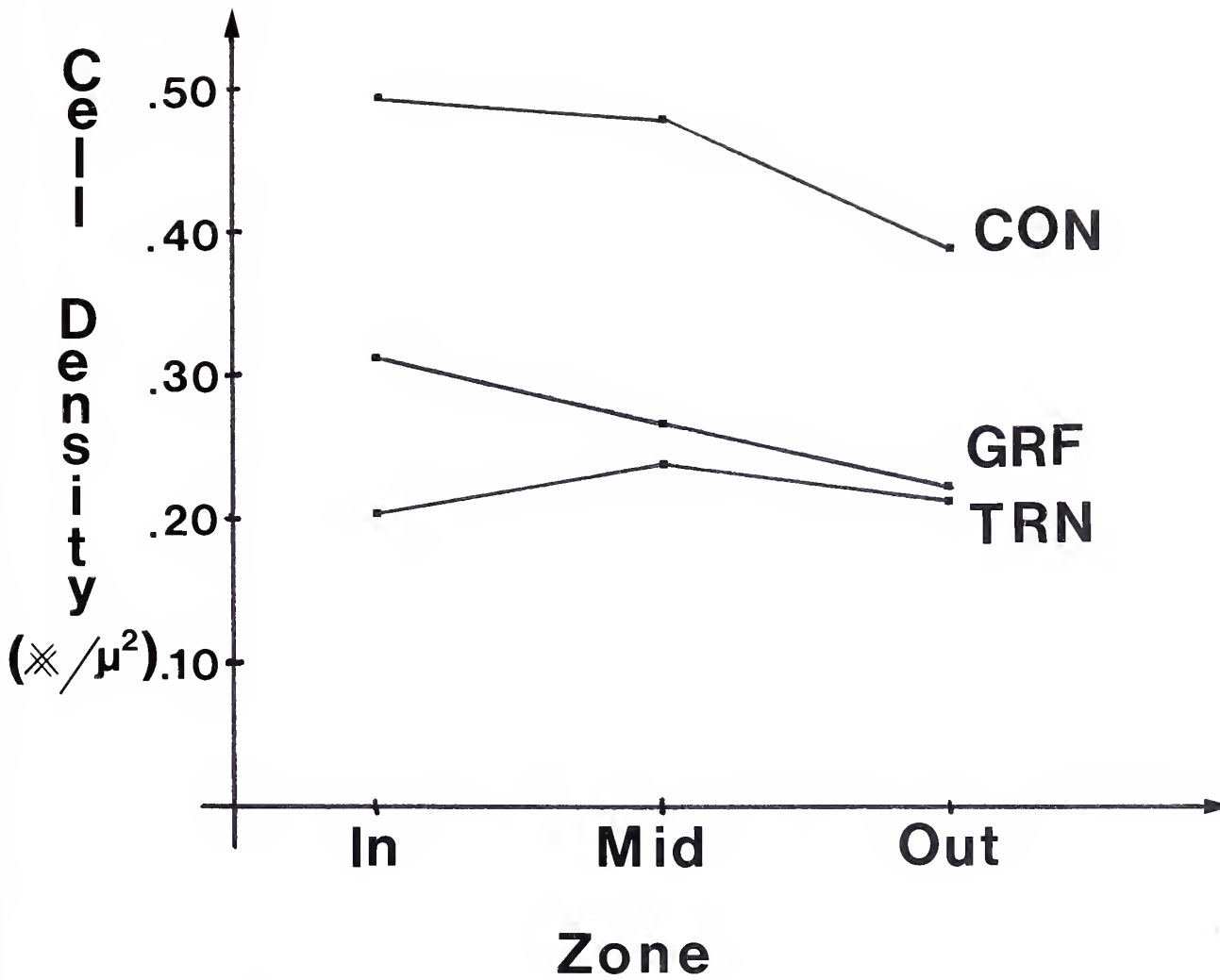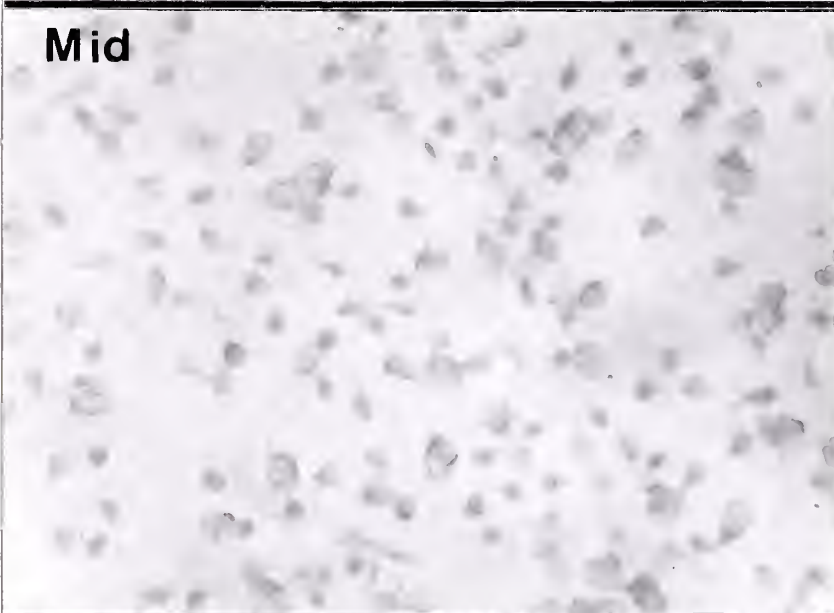
FIGURE 19:

Photomicrographs illustrating the natural cell density decrease from inner, to middle, to outer retinal zones in a control wholemount. Magnification for all micrographs is identical(320x). Comparison with experimental animals in Figures 20 and 21 is made.
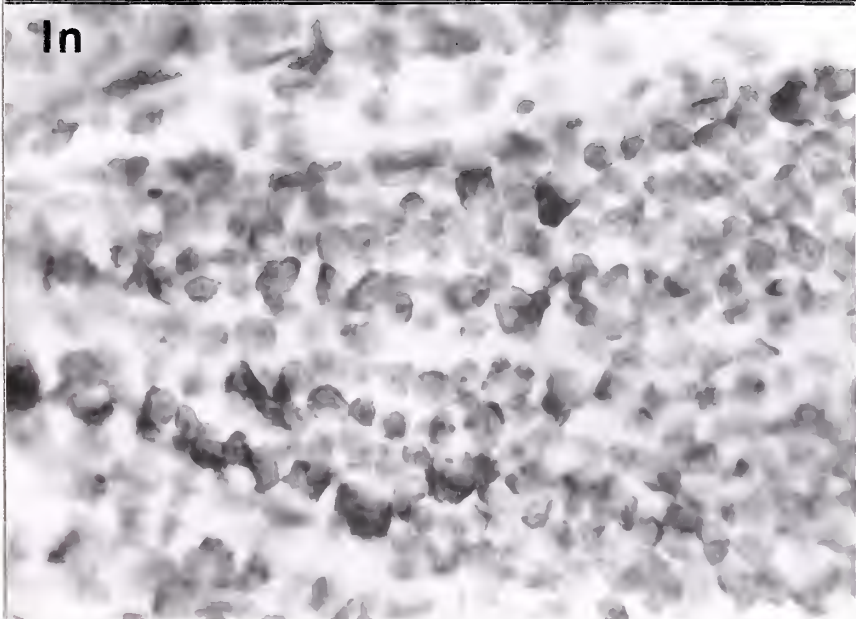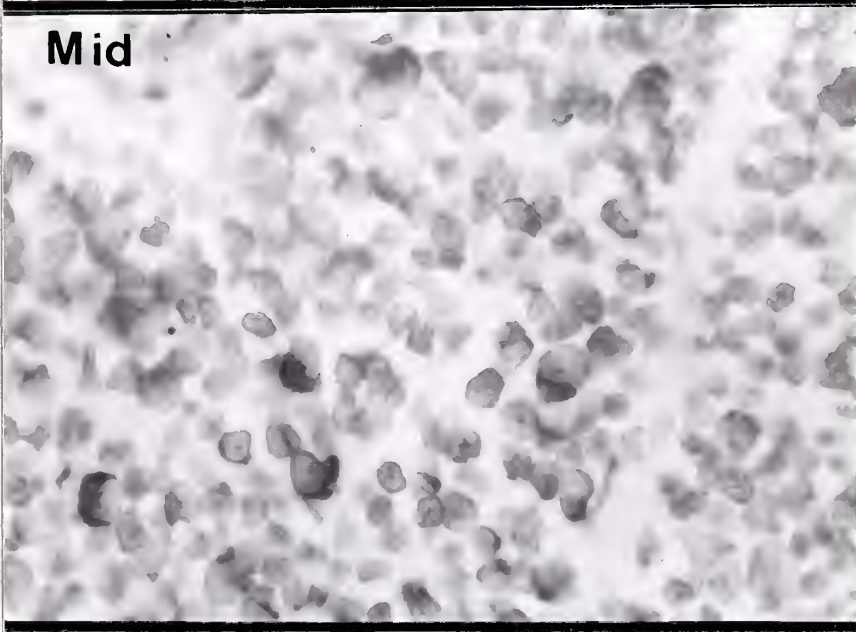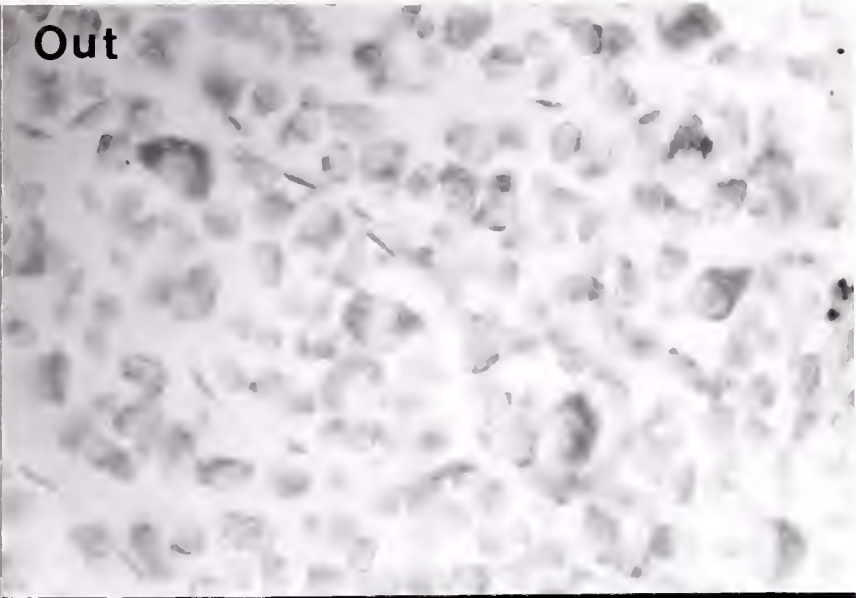
FIGURE 20:

Photomicrographs illustrating transection alone retinal cell density as low and relatively constant across the wholemount. There is actually a small increase in moving from inner to middle retinal zones. Magnification for all micrographs is identical and equal to that in Figures 19 and 21 (320x).
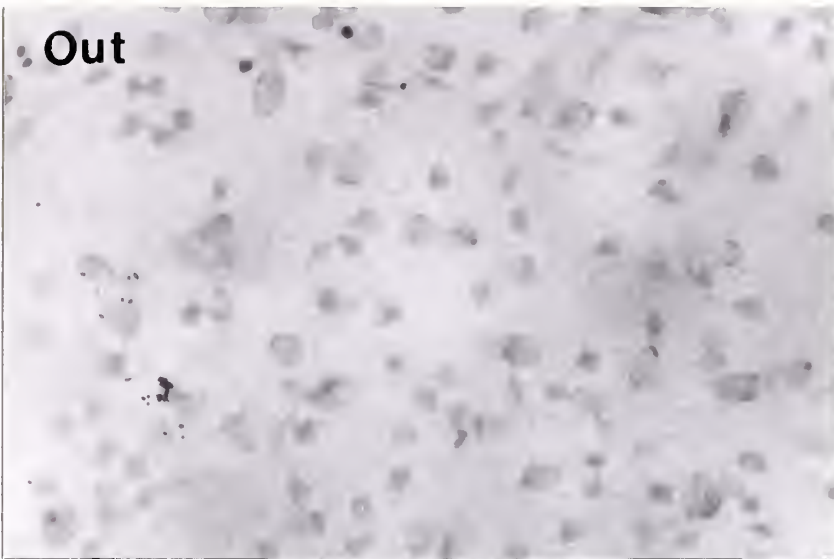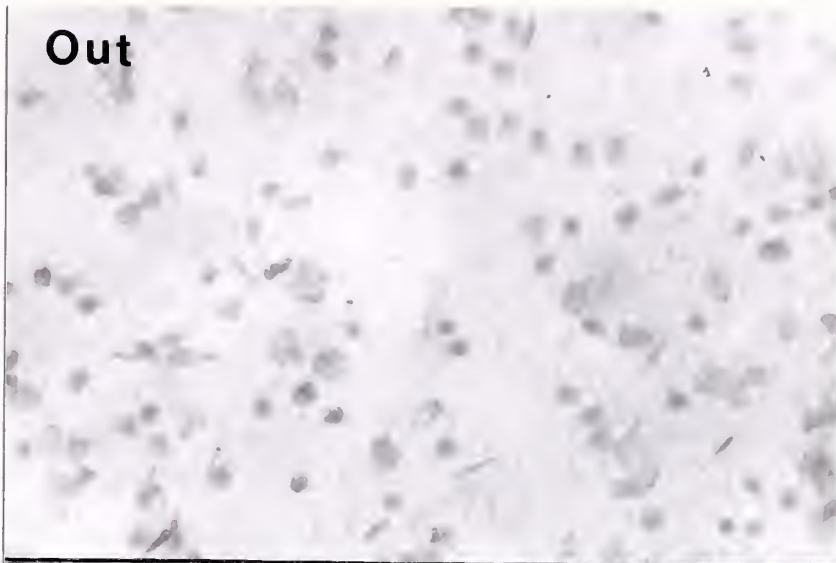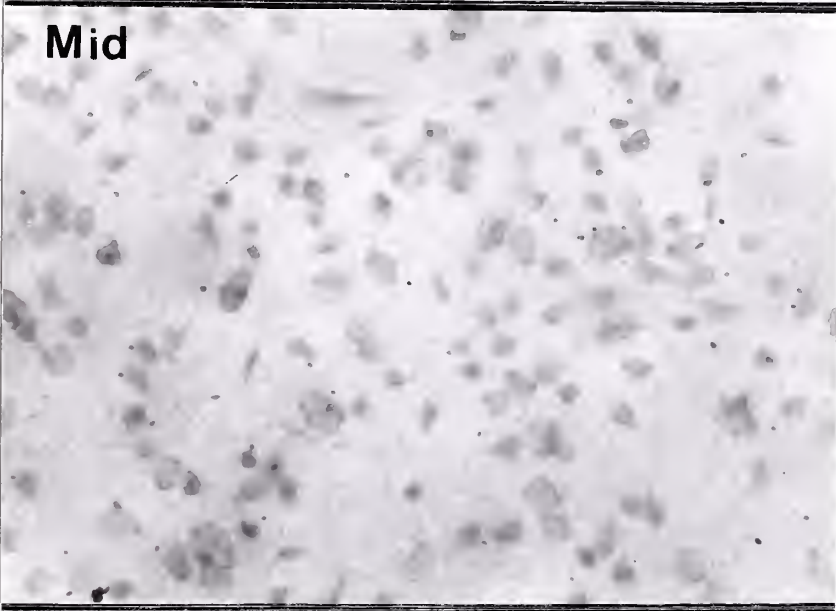
Out

Mid

In
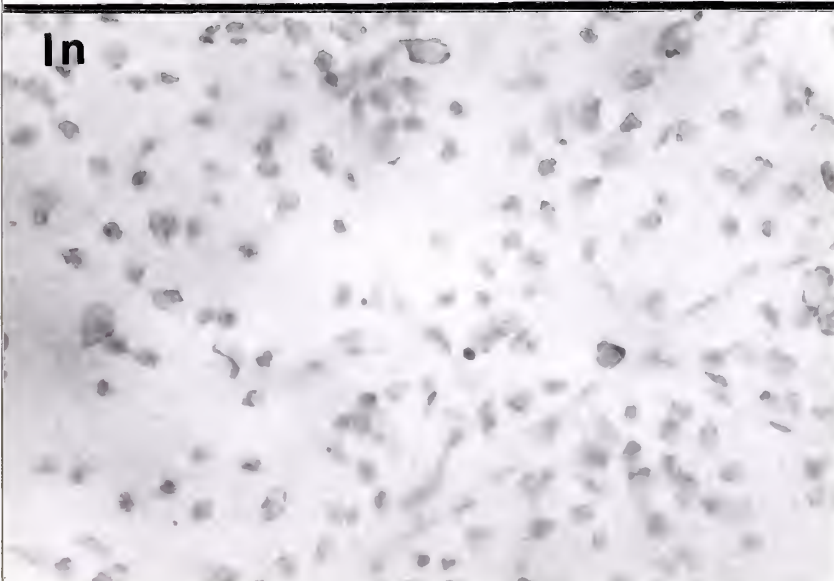
FIGURE 21:

Photomicrographs illustrating grafted retinal cell density decrease from inner to middle zone. A further small decrease in moving to the outer zone is also noted as with controls. Magnification for all micrographs is identical and equal to that in Figures 19 and 20 (320x).
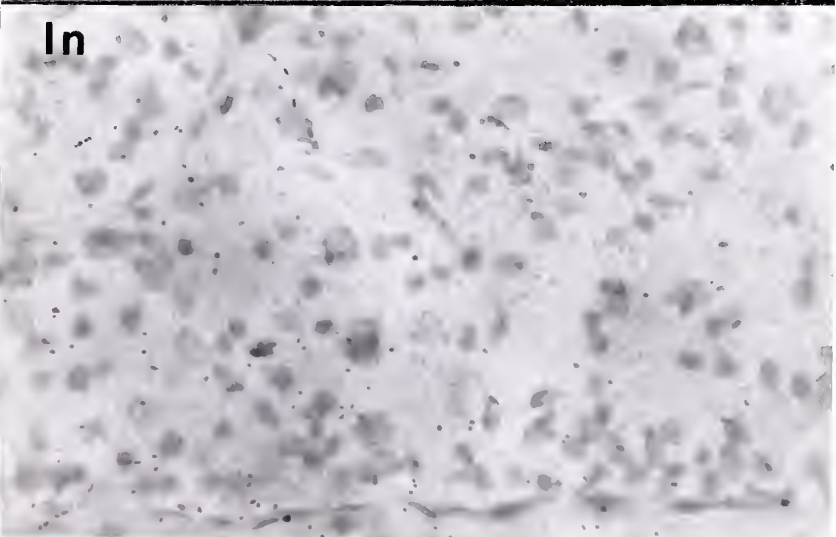
FIGURE 22:

Electron micrograph of optic nerve one month following a complete intracranial transection alone. Section is from proximal stump of nerve(retinal side) approximately 1 mm proximal to site of transection. A group of normal appearing axons from within the dashed box is shown at higher magnification in the inset. Although there are axons in various stages of degeneration, others(inset) have normal myelination and axoplasm.

Main micrograph is 15,000x and size bar = 1 micron.

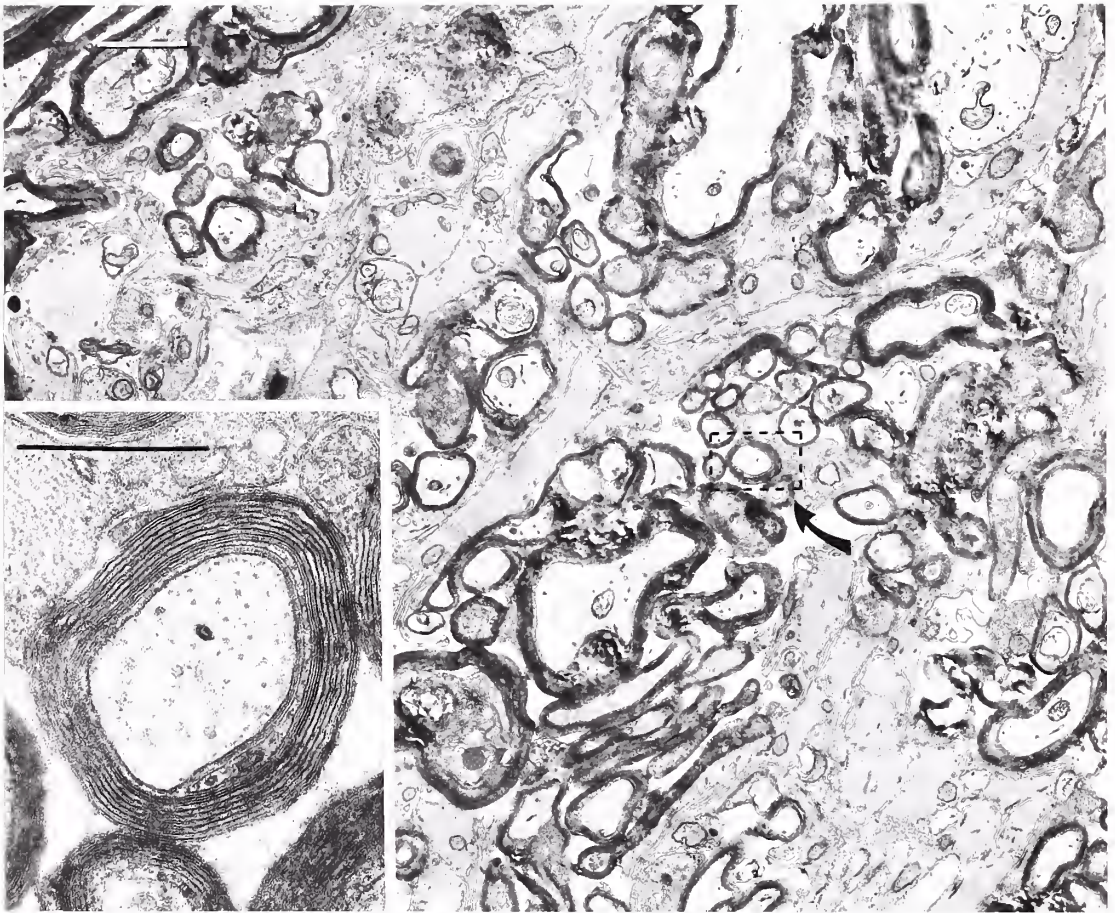Inset micrograph is 100,000x and size bar = 0.5 microns.

FIGURE 23:

Electron micrograph of optic nerve from intracranial transection alone animal at three months survival. Section is from proximal nerve stump at a position midway between the optic nerve head and optic foramen.

A) Low power micrograph from central portion of cross-sectional area of the optic nerve. A centrally located blood vessel(bv) is seen with several healthy small myelinated axons(arrows). (5,000x)

B) A healthy appearing myelinated axon from A). The area surrounding the axon is largely filled with astrocytic processes. Normal axoplasmic contents are noted: neurofilaments(nf), microtubules(mt) and mitochondria(m). (36,000x)

C) High power view showing probable remyelination of optic axon. Only three concentric layers of myelin(arrowhead) seen with wide periodicity. Axoplasmic contents are normal appearing as well: neurofilaments(nf) and Microtubules(mt). (150,000x)
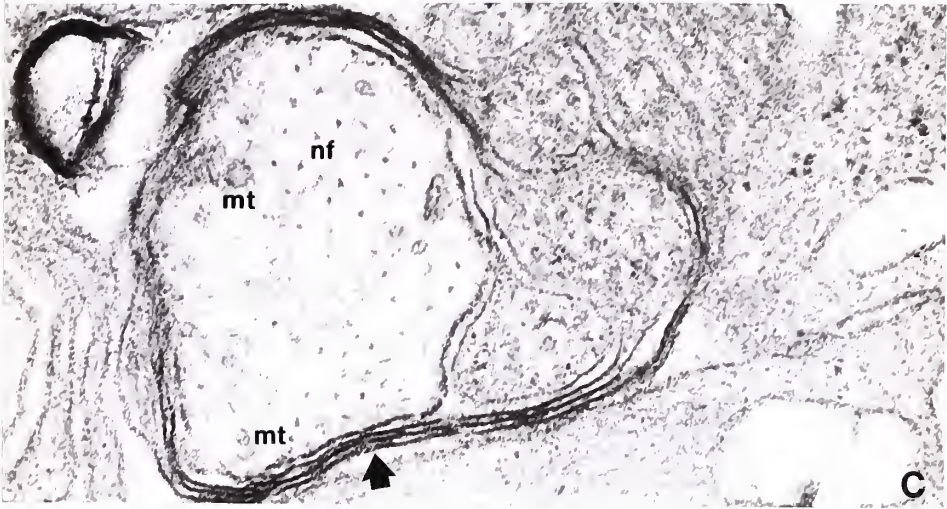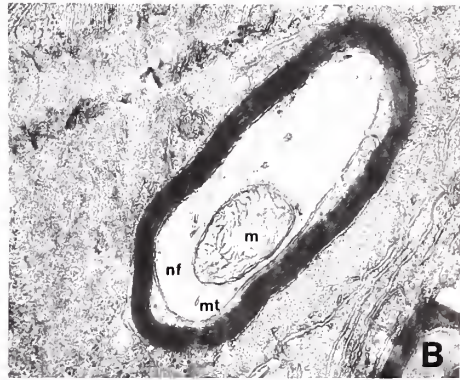
FIGURE 24:

Electron micrograph of optic nerve from intracranial transection alone animal after three months survival. This micrograph is from the same proximal nerve segment as the previous figure but at the site of intracranial transection. A myelinated axon(open arrow) is seen among a cross-sectional area largely filled with astrocytic processes some of which are labeled with an (a). At least two unmyelinated axons(solid arrows) with one cut longitudinally(curved arrow) are seen in this axial section. A longitudinally oriented axon is usually not found in the normal optic nerve at this position midway between optic chiasm and foramen. Yet, at this level in these transverse sections many such axons were found. They may represent sprouting(unmyelinated) axons turning back from the transection site as if there were a barrier to rectilinear growth. (40,000x)
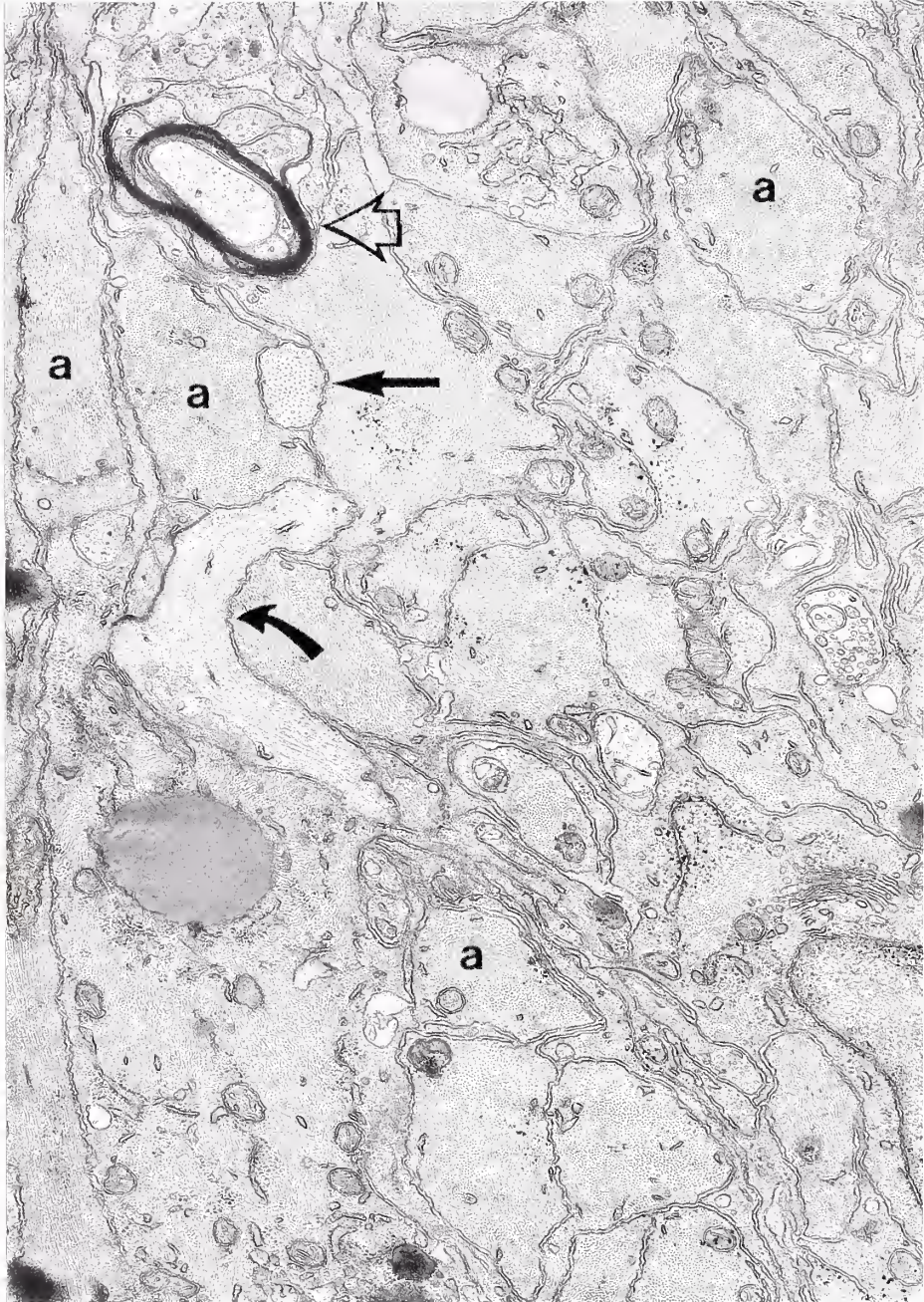
LIST OF TABLES

1.   The individual retinal wholemount data for cell density (# cells/ sq. micron) and mean cell areas (sq. microns). BASE corresponds to the wholemount name, and GROUP refers to control(CON), transection alone(TRN), and grafted animals(GRF). The columns in order across the top represent; overall density, inner zone density, middle zone density, outer zone density, overall mean area, inner zone mean area, middle zone mean area, and outer zone mean area.

2.   The combined average of the means in Table 1 by group. The standard deviations are also presented. Headings and abreviations are the same as above.

3.   Parametric Duncan-Waller test for difference of mean cell density by zone and group for the area class 21-30 sq. microns. Nine groups are compared: control inner zone(COIN), control middle zone(COMD), control outer zone(COOT), transection inner zone(TRIN), transection middle zone(TRMD), transection outer zone (TROT), grafted inner zone(GRIN), grafted middle zone(GRMD), and grafted outer zone(GROT). This analysis was run on all 10 sq. micron area classes.

4.   Nonparametric analyses comparing the inner zone cell density(INDNS) between transection(TRN) and grafted(GRF) animals using Wilcoxon, Kruskal-Wallis, and Median 2-sample tests.

BASE	GROUP	OVDNS	INDNS	MIDDNS	OUTDNS	OVMAR	INMAR	MIDMAR	OUTMAR
RET2	CON	0.60686	0.77249	0.64106	0.50683	40.0695	39.7965	41.3153	37.9678
RET4	CON	0.33931	0.30031	0.40238	0.31190	39.9423	40.2762	40.3402	35.9624
RE15	CON	0.37796	0.39279	0.41818	0.33814	36.1173	38.1115	35.6526	34.4296
RE16	CON	0.48301	0.55296	0.51913	0.42294	33.9985	32.3066	34.0089	35.7230
RE18	CON	0.40410	0.44330	0.40574	0.36901	34.7907	37.0000	35.1023	32.7868
RET9	TRN	0.17007	0.17115	0.17884	0.16311	23.9306	24.1932	25.2517	22.5886
RE14	TRN	0.26244	0.29958	0.28449	0.23152	22.1412	21.5306	21.6459	23.6378
RM1R	TRN	0.17885	0.17222	0.17107	0.19344	42.8571	48.8497	43.7958	36.8878
RM2R	TRN	0.22111	0.21222	0.22090	0.23017	28.2583	33.6942	27.7734	25.6577
RET1	GRF	0.31338	0.39852	0.31552	0.26625	23.2727	22.9645	23.0320	24.1071
RET5	GRF	0.26019	0.32758	0.28931	0.21162	25.6329	24.6702	26.2349	25.9741
RE17	GRF	0.29240	0.36413	0.28586	0.23617	16.9463	15.4598	17.0496	18.3502
rm11	GRF	0.21165	0.22064	0.22320	0.19704	39.7476	43.5882	39.3209	37.4774
RM2L	GRF	0.22138	0.19537	0.21169	0.23831	36.1756	39.6914	39.0221	33.3281
RET3	GRF	0.29810	0.38289	0.32528	0.25312	19.9746	18.4780	20.1647	20.2789
RET7	GRF	0.20681	0.30213	0.21635	0.16775	27.3592	25.1587	28.8073	28.6364

T A B L E 1

VARIABLE	MEAN	STANDARD DEVIATION
----------------- GROUP=CON -----------------		
OVDNS	0.44224600	0.10599894
INDNS	0.49237000	0.18121082
MIDDNS	0.47729800	0.10343609
OUTDNS	0.38976400	0.07740101
OVMAR	36.78366000	2.86124067
INMAR	38.69816000	5.06737105
MIDMAR	37.28386000	3.30678465
OUTMAR	35.37392000	1.92232341
----------------- GROUP=GRF -----------------		
OVDNS	0.25798714	0.04429468
INDNS	0.31503571	0.07906650
MIDDNS	0.26674429	0.04855716
OUTDNS	0.22432286	0.03422806
OVMAR	27.00127143	8.31095553
INMAR	27.14440000	10.54354755
MIDMAR	27.66450000	8.73856824
OUTMAR	26.87868571	6.85333801
----------------- GROUP=TRN -----------------		
OVDNS	0.20811750	0.04252034
INDNS	0.21579250	0.06030098
MIDDNS	0.21382500	0.05194721
OUTDNS	0.20456900	0.03278450
OVMAR	29.29680000	9.39783316
INMAR	32.06692500	12.34664935
MIDMAR	29.61670000	9.78147074
OUTMAR	26.69297500	6.81486952

TABLE 2

GENERAL LINEAR MODELS PROCEDURE

WALLER-DUNCAN K-RATIO T TEST FOR VARIABLE: B3
NOTE: THIS TEST MINIMIZES THE BAYES RISK UNDER ADDITIVE LOSS
      AND CERTAIN OTHER ASSUMPTIONS

        KRATIO=100   DF=39   MSE=9.1E-04   F=3.138
        CRITICAL VALUE OF T=2.25
        MINIMUM SIGNIFICANT DIFFERENCE=.04233

            CELL SIZES ARE NOT EQUAL.
            HARMONIC MEAN OF CELL SIZES=5.06024

MEANS WITH THE SAME LETTER ARE NOT SIGNIFICANTLY DIFFERENT.

WALLER	GROUPING			MEAN	N	GROUP
	A			0.12676	5	COMD
	A					
B	A			0.12325	5	COIN
B	A					
B	A	C		0.09510	5	COOT
B		C				
B		C		0.08116	7	GRIN
B		C				
B		C		0.08107	7	GRMD
		C				
		C		0.07395	4	TROT
		C				
		C		0.07022	7	GROT
		C				
		C		0.06975	4	TRMD
		C				
		C		0.05647	4	TRIN

TABLE 3

ANALYSIS FOR VARIABLE INDNS CLASSIFIED BY VARIABLE GROUP

ANALYSIS OF VARIANCE

LEVEL	N	MEAN	AMONG MS	WITHIN MS
			0.0250707	0.00537974
TRN	4	0.21		
GRF	7	0.31	F VALUE	PROB>F
			4.66	0.0592

WILCOXON SCORES (RANK SUMS)

LEVEL	N	SUM OF SCORES	EXPECTED UNDER HO	STD DEV UNDER HO	MEAN SCORE
TRN	4	13.00	24.00	5.29	3.25
GRF	7	53.00	42.00	5.29	7.57

WILCOXON 2-SAMPLE TEST (NORMAL APPROXIMATION)
(WITH CONTINUITY CORRECTION OF .5)
S=   13.00   Z=-1.9843   PROB >IZI=0.0472

T-TEST APPROX. SIGNIFICANCE=0.0753

KRUSKAL-WALLIS TEST (CHI-SQUARE APPROXIMATION)
CHISQ=   4.32   DF= 1   PROB > CHISQ=0.0376

MEDIAN SCORES (NUMBER POINTS ABOVE MEDIAN)

LEVEL	N	SUM OF SCORES	EXPECTED UNDER HO	STD DEV UNDER HO	MEAN SCORE
TRN	4	0.00	1.82	0.83	0.00
GRF	7	5.00	3.18	0.83	0.71

MEDIAN 2-SAMPLE TEST (NORMAL APPROXIMATION)
S=   0.00   Z=-2.1822   PROB >IZI=0.0291

MEDIAN 1-WAY ANALYSIS (CHI-SQUARE APPROXIMATION)
CHISQ=   4.76   DF= 1   PROB > CHISQ=0.0291

TABLE 4

Aguayo, A., David, S. and Bray, G. (1981) Influences of the glial environment on the elongation of axons after injury: transplantion studies in adult rodents. J. Exp. Biol 95:231-240.

Aguayo, A., Dickson, R., Trecarten, J., Attiwell, M., Bray, G., and Richardson, P. (1978) Ensheathment and myelination of regenerating PNS fibers by transplanted optic nerve glia. Neurosci. Lett. 9:97-104.

Akagawa, K. and C. Barnstable (1984) Monoclonal antibodies that detect cell type and laminar differences in rat retina. Soc. Neurosci. Abstr. 10:21.

Allcutt, D., Berry, M., and Sievers, J. (1984a) A qualitative comparison of the reactions of retinal ganglion cell axons to optic nerve crush in neonatal and adult mice. Dev. Brain Res. 16:219-231.

Allcutt, D., Berry, M., and Sievers, J. (1984b) A quantitative comparison of the reactions of retinal ganglion cells to optic nerve crush in neonatal and adult mice. Dev. Brain Res. 16:231-240.

Ames, A., and D. Pollen (1969) Neurotransmission in central nervous tissues: a study of isolated rabbit retina. J. Neurophys. 32:424-442.

Anderson, D. (1970) Vascular supply of the optic nerve of primates. Amer. Journal of Ophthalmol. 70:341-357.

Anderson, D. (1973) Ascending and descending optic atrophy produced experimentally in squirrel monkeys. Amer. J. Ophthamol. 7:693-702.

Arenella, L. and R. Herndon (1983) Mature oligodendrocytes have the capacity to divide following experimental demyelination in the adult CNS. Soc. Neurosci. Abstr. 9:768.

Athwal, S. Chakraboty, G., Zanakis, M. and Ingoglia, N. (1984) Posttranslational protein modification by amino acid addition following injury to rat sciatic and optic nerve. Soc. Neurosci. Abstr. 10:1031.

Balkerna, G. and Drager, U. (1984) Monoclonal antibodies against components of the mouse retina. Soc. Neurosci. Abstr. 10:21.

Benfey, M., and A. Aguayo (1982) Extensive elongation of axons from rat brain into peripheral nerve grafts. Nature 296:150-152.

Bernstein, J. and M. Bernstein (1971) Axonal regeneration and formation of synapses proximal to the site of lesion following hemisection of the rat spinal cord. Exp. Neurol. 30:336-351.

Berry, M. and A. Riches (1974) An immunological approach to regeneration in the central nervous system. Br. Med. Bull. 30:135-140.

Bjorklund, A. and U. Stenevi (1979) Regeneration of monoaminergic and cholinergic neurons in the mammalian central nervous system. Physiol. Rev. 89:62-100.

Bock, S., Snipes, G., Norden, J., and Freeman, J. (1984) Developmental program of protein expression in rat retinal ganglion cells. Soc. Neurosci. Abstr. 10:1030.

Brodal, A. (1940) Modification of the "Gudden method" for study of cerebral localization. Arch. Neurol. Psychiat. 43:46-58.

Bugge, J. (1970) The contribution of the stapedial artery to the cephalic arterial supply in muroid rodents. Acta. Anatomica 76:313-336.

Brooks, B., & R. Jung (1973) Neuronal physiology of the visual cortex. In R. Jung (ed.): Handbook of sensory physiology. Vol II, Berlin-Heidelberg-New York: Springer-Verlag, pp. 326-440.

Cajal, Ramon y, S. (1928) Degeneration and Regeneration in the Nervous System, vol. 2. New York:Oxford University Press (translated by R.M. May).

Clifford-Jones, R., Landon, D., and McDonald, W.I. (1980) Remyelination during optic nerve compression. Journal of Neurological Science. 46:239-243.

Cole, M. (1969) Retrograde degeneration of axon and soma in the nervous system. In G.H. Bourne (ed): The Structure and Function of Nervous Tissue. vol 1. New York: Academic Press, p. 269.

DaSilva, C., Dikkes, P., Madison, R., Greatorex, D., and Sidman, R. (1984) Laminin gel stimulates axonal regeneration in vivo. Soc. Neurosci. Abstr. 10:283.

David, S. and A. Aguayo (1981) Axonal elongation into peripheral nervous system "bridges" after central nervous system injury in adult rats. Science 214:931-933.

Davis, R. and S. Benloucif (1981) Behavioral investigation of neurotoxicity: the effects of colchicine, lumicolchicine and vincristine sulfate on goldfish optic nerve regeneration. Neurotoxicology 2:419-430.

Dreher, S., Potts, R. and Bennett, M. (1983) Evidence that the early postnatal reduction in the number of rat retinal ganglion cells is due to a wave of ganglion cell death. Neurosci. Lett. 36:255-260.

Dunn, G. (1971) Mutual contact inhibition of extension of chick sensory nerve fibers in vitro. J. Comp. Neurol. 143:491-507.

Eayrs, J.T. (1952) Relationship between ganglion cell layer of retina and the optic nerve in the rat. Br. Journ. Ophthamol. 36:453-459.

Engh, C.A. and B.H. Schofield (1972) A review of the central response to peripheral nerve injury and its significance in nerve regeneration. J. Neurosurg. 37:195-203.

Eysel, U. and L. Peichl (1985) Regenerative capacity of retinal axons in the cat, rabbit and guinea pig. Exp. Neurol. 88:757-766.

Fawcett, J., O'Leary, D. and Cowan, W. (1984) Activity and the control of ganglion cell death in the rat retina. Proc. Natl. Acad. Sci. USA 81:5589-5593.

Fulcrand, J., and A. Privat (1977) Neuroglial reactions secondary to Wallarian degeneration in the optic nerve of postnatal rat: Ultrastructural and quantitative study. J. Comp. Neurol. 176:189-224.

Goldberg, S. (1976) Central nervous system regeneration and ophthalmology. Survey of Ophthal. 20:261-272.

Goldberg, S. and B. Frank (1979) The guidance of optic axons in the developing and adult mouse retina. Anatomical Record 193:763-774.

Goldberg, S. and B. Frank (1981) Do young axons regenerate better than old axons? Exp. Neurol. 74:245-259.

Grafstein, B., and N. Ingoglia (1982) Intracranial transection of the optic nerve in adult mice:preliminary observations. Exp. Neurol. 76:318-330.

Guth, L., Barrett, C., Donati, E., Deshpande, S., and Albuquerque, E. (1981) Histological reactions and axonal regeneration in the transected spinal cord of hibernating squirrels. J. Comp. Neurol. 203:297-308.

Gutman, E. (1945) The reinervation of muscle by sensory nerve fibers. J. Anat. 79:1-8.

Hadani, M., Harel, A., Solomon, A., Belkin, M., Lavie, V. and Schwartz, M. (1984) Substances originating from the optic nerve of neonatal rabbit induce regeneration-associated response in the injured optic nerve of adult rabbit. Proc. Natl. Acad. Sci. USA 81:7965-7969.

Harris, W., Hold, C., Smith, T., and Gallenson, N. (1985) Growth cones of developing retinal cells in vivo, on culture surfaces, and in collagen matrices. J. Neurosci. Res. 13:101-122.

Hinds, J., and P. Hinds (1974) Early ganglion cell differentiation in the mouse retina: an electron microscopic analysis utilizing serial sections. Dev. Biology 37:381-416.

Hubel, D., and T. Wiesel (1962) Receptive fields, binocular interaction and functional architecture in the cat's visual cortex. J. Physiol. 160: 106-154.

Hughes, A. (1975) A quantitative analysis of cat retinal ganglion cell topography. J. Comp. Neurol. 163:107-128.

Ignatius, M., Gebicke-Harter, P., Shilling, J., Skene, J., and Shooter, E. (1985) Evidence that a nerve injury induced 37kDa protein is a form of apolipoprotein. Soc. Neurosci. Abstr. 10:1252.

Ignatius, M., Muller, H., Skene, J. and Shooter, E. (1984) Purification and characterization of a denervation induced nerve sheath released protein. Soc. Neurosci. Abstr. 10:1029.

Jacobson, M. (1978) Developmental Neurobiology, 2nd Ed. New York: Plenum Press.

James, G.R. (1933) Degeneration of ganglion cells following axonal injury. Arch. Ophthalmol. 9:338-343.

James, R. and G. Bounds (1955) The blood vessels of the rat's eye. American Journal of Anatomy 96:357-373.

Kalil, KJ. and T. Reh (1982) A light and electron microscopic study of regrowing pyramidal tract fibers. J. Comp. Neurol. 211:265-275.

Keating, M. (1976) The formation of visual neuronal connections: an appraisal of the present status of the theory of neuronal specificity. In G. Gottlieb (ed): Studies on the development of behavior and the nervous system. Vol. 3, New York: Academic Press, pp. 59-103.

Keirstead, S., Vidal-Sanz, M., Rasminsky, M., Aguayo, A., Levesque, M. and So K.-F. (1985) Responses to visual stimuli of rat retinal ganglion cells regenerating axons into peripheral nerve grafts. Soc. Neurosci. Abstr. 11:254.

Kiernan, J.A. (1979) Hypotheses concerned with axonal regeneration in the mammalian nervous system. Biol. Rev. 54:155-197.

Kuffler, S.W. (1953) Discharge patterns and functional organization of mammalian retina. J. Neurophys. 16:37-68.

Kupfer, C. (1953) Retinal ganglion cell degeneration following chiasmal lesion in man. Arch Ophthal. 70:256-263.

Lanners, H. and B. Grafstein (1980) Early stages of axonal regeneration in the goldfish optic tract: an electron microscopic study. Journal of Neurocytology 9:733-751.

Lavie, V., Sharma S., Harel, A., Lobel, D., Solomon, A., Daron, A., Belkin, M., and Schwartz, M. (1985) Substances originating from growing nerve induce morphological responses characteristic of regeneration in injured optic nerve of adult rabbit. Soc. Neurosci. Abstr. 10:1252.

LeGros, Clark, W. (1942a) The problem of neuronal regeneration in the central nervous system. I. The influence of spinal ganglia and nerve fragments grafted in brain. J. Anat. (Lond.) 77:20-48.

LeGros Clark, W. (1942b) The problem of neuronal regeneration in the central nervous system. II. The insertion of peripheral nerve stumps into brain. J. Anat. (Lond.) 77:251-259.

Leinfelder, P.J. (1938) Retrograde degeneration in the optic nerve and retinal ganglion cells. Trans. Amer. Ophthal. Soc. 36:307-315.

Lim, R. and J. Miller (1983) In vivo effect of glia maturation factor on central regeneration. Soc. Neurosci. Abstr. 9:768.

Liu, C. (1954) Time pattern retrograde degeneration after trauma of central nervous system. In W. Windle (ed): Regeneration in the central nervous system. Springfield:Thomas.

Lundborg, G., Lango, F., and Varon, S. (1982) Nerve regeneration model and trophic factors in vivo. Brain Res. 232:157-161.

Madison, R., DaSilva, C., Dikkes, P. Chiu, T-H., and Sidman, R.(1985)Increased rate of peripheral nerve regeneration using bioresorbable nerve guides and a Laminin-containing gel. Exp. Neurol. 88:767-772.

Madison, R., Moore, M., and Sidman, R. (1984) Retinal ganglion cells and axons survive optic transection. Intern J. Neurosci 23:15-32.

Mark, R.F. (1975) Topography and toplogy in functional recovery of regenerated sensory and motor systems. In Symposium on Cell Patterning. (CIBA Foundation Symposium No. 29). New York: Elsevier.

McCaffrey, C., Raju, T., and Bennett, M. (1985) Retinal ganglion cell survival is mediated by cell contact with immature rat astroglia. Neurosci. Lett. 57:319-324.

McConnell P. and M. Berry (1982) Regeneration of ganglion cell axons in the adult mouse retina. Brain Res. 241:362-365.

McGeer, P., Eccles, J., and McGeer, E. (1978) Molecular neurobiology of the mammalian brain. New York: Plenum Press.

McQuarrie, I. (1985) Stages of axonal regeneration following optic nerve crush in goldfish: Contrasting effects of conditioning nerve lesions and intraocular acetoxycyloheximide injections. Brain Res. 333:247-253.

Meiri, H., and B. Grafstein (1984) Local application of calcium-modulating agents to crushed goldfish optic nerve modifies visual recovery. Exp. Neurol. 83:403-413.

Miller, N., and M. Oberdorfer (1981) Neuronal and neuroglial responses following retinal lesions in the neonatal rat. J. Comp. Neurol. 202: 493-504.

Misantone, L., Barron, K., Gershenbaum, M., Cipolla, V., Zanakis, M., and Murray, M. (1981) Effect of optic nerve crush on retinal ganglion cells in hooded rats. Soc. for Neurosci. Abstr. 7:681.

Misantone, L., Gershenbaum, M., and Murray, M. (1984) Viability of retinal ganglion cells after optic nerve crush in rats. J. Neurocytology 13:449-465.

Moore, R.Y. (1980) Regeneration in the mammalian nervous system. Ann. N.Y. Acad. Sci. 339:102-114.

Muller, H., Ignatius, M., Gebicke-Harter P., Hangen, D., and Shooter, E. (1985) Expression of specific non-neuronal protein defines distinct "growth states" of regenerating and non-regenerating nerves in mammals. Soc. Neurosci. Abstr. 10:1252.

Murray, M. (1976) Regeneration of retinal axons into the goldfish optic tectum. J. Comp. Neurol. 168:175-196.

Murray, M. (1982) A quantitative study of regenerative sprouting by optic axons in goldfish. J. Comp. Neurol. 209:352-362.

Neumann, D., Yerushalmi, A., and Schwartz, M. (1983) Inhibition of nonneuronal cell proliferation in the goldfish visual pathway affects the regenerative capacity of the retina. Brain Res. 272:237-245.

Pei, Y. and Rhodin, J. (1970) The prenatal development of the mouse eye. Anatomical Record 168:105-126.

Pellegrino, R., Politis, M. and Ritchie J. (1982) Functional correlates of reactive glial protein synthesis in degenerating rat optic nerve. Soc. Neurosci. Abstr. 8:760.

Perry, V., Henderson, Z., and Linden R. (1983) Postnatal changes in retinal ganglion cell and optic axon populations in the pigmented rat. J. Comp. Neurol. 219:356-368.

Politis, M. (1985) Dynamics of induction of axon regeneration in rat optic nerve. Soc. Neurosci. Abstr. 10:1254.

Politis, M., Ederle, K. and Spencer, P. (1982) Tropism in nerve regeneration in vivo. Attraction of regenerating axons by diffusible factors derived from cells in distal nerve stumps of transected peripheral nerve. Brain Res. 253:1-12.

Politis, M. and Spencer, P. (1982) Regeneration of rat optic axons into adjacent peripheral nerve grafts. Soc. Neurosci. Abstr. 8:761.

Polyak, S. (1941) The Retina. Chicago: University of Chicago Press.

Polyak, S. (1957) The Verterbrate Visual System. Chicago: University of Chicago Press.

Quigley, H., Davis, E., and Anderson, D. (1977) Descending optic nerve degeneration in primates. Invest. Ophthal. Vis. Sci. 16:841-849.

Redshaw, J., and M. Bisby (1981) Fast axonal transport of proteins in rat retinal ganglion cells following axotomy. Fed. Proc. 40:302.

Reh, T. and M. Constantine-Paton (1985) Growth cone-target interactions in the frog retinotectal pathway. J. Neurosci. Res. 3:89-100.

Reh, T. and Kalil, K. (1982) Functional role of regrowing pyramidal tract fibers. J. Comp. Neurol. 211:276-283.

Reier, P., Stensaas, L, and Guth, L. (1981) The astrocytic scar as an impediment to regeneration in the central nervous system. In C.C. Kao, R.P. Bunge, P.J. Reier and S. Griller (eds): Fundamentals of spinal cord reconstruction. New York: Raven Press.

Reier, P.J. and Webster, H. (1974) Regeneration and remyelination of Xenopus tadpole optic nerve fibers following transection or crush. Journal of Neurocytology 3:591-618.

Richardson, P., Issa, V., and Aguayo, A. (1984) Regeneration of long spinal axons in the rat. J. Neurocytol. 13:165-182.

Richardson, P. Issa, V., and Shermie, S. (1982) Regeneration and retrograde degeneration of axons in the rat optic nerve. J. Neurocytol. 11:949-966.

Rowe, M.H. and J. Stone (1976) Conduction velocity groupings among axons of cat retinal ganglion cells, and their relationship to retinal topograghy. Exp. Brain Res. 25:339-357.

Salame, C., and R. Dunn (1984) Characteristics of CNS axonal regeneration into sciatic nerve implants in rats. Soc. Neurosci. Abstr. 10:1084.

Schwartz, M., Hadani, M., Harel,A., Solomon, A., Lavie, V., Belkin, M., and Rachailovich, I. (1984) Regenerative responses are induced by signal of external origin implanted into severed optic nerve of adult rabbits. Soc. Neurosci. Abstr. 10:281.

Seckel, B., Chiu,T., Nyilas, E., and Sidman, R. (1984) Nerve regeneration through synthetic biodegradable nerve guides: Regulation by the target organ. Plast. and Reconstr. Surg. 74:173-181.

Sefton, A. and Lam K. (1984) Quantitative and morphological studies on developing optic axons in normal and enucleated albino rats. Exp. Brain Res. 57:107-117.

Sengelaub, D., Windrem, M., and Finlay, B. (1983) Increased cell number in the adult hamster retinal ganglion cell layer after early removal of one eye. Exp. Brain Res. 52:269-276.

Shepherd, G.M. (1974) The Synaptic Organization of the Brain. New York: Oxford University Press.

Silver, J. (1984) Studies on the factors that govern directionality of axonal growth in the embryonic optic nerve and at the chiasm of mice. J. Comp. Neurol 223:238-251.

Skoff, R., Toland, D. and Nast, E. (1980) Pattern of myelination and distribution of neuroglial cells along the developing optic system of the rat and rabbit. J. Comp. Neurol. 191:237-253.

Skene, J. and E. Shooter (1983) Denervated sheath cells secrete a new protein after injury. Proc Natl. Acad. Sci. USA 80:4169-4173.

Smalheiser, N., Crain, S. and Bernstein, M. (1981) Development of ganglion cells and their axons in organized cultures of fetal mouse explants. Brain Res. 204:159-178.

Smalheiser, N., Crain, S. and Reid, L. (1984) Laminin as a substrate for retinal axons in vitro. Dev. Brain Res. 12:136-140.

Snipes, G. and J. Freeman (1984) Characterization of the 37kDa protein associated with nerve development and injury. Soc. Neurosci. Abstr. 10:1029.

So, K.-F. and A. Aguayo (1984) Ganglion cell axons regenerate along segments of peripheral nerve transplanted into the retina of adult rats. Soc. Neurosci. Abstr. 10:1083.

So, K.-F. and A. Aguayo (1985) Lengthy regrowth of cut axons from ganglion cells after peripheral nerve transplantation into retina of adult rats. Brain Res. 328:349-354.

Sparrow, J., McGuinness, C. Schwartz, M. and Grafstein, B. (1984) Antibodies to gangliosides inhibit goldfish optic nerve regeneration in vivo. J. Neurosci. Res. 12:233-243.

Stein-Izsak, C., Solomon, A., Neumann, D., Belkin, M., Rubinstein, M., Schwartz, M. (1985) Molecular aspects of optic nerve regeneration in regenerative and non-regenerative systems. Soc. Neurosci. Abstr. 10:128.

Stone, J. (1966) The nasotemporal division of the cat's retina. J. Comp. Neurol. 126:585-600.

Stone, J. and Y. Fukuda (1974) Properties of cat retinal ganglion cells: a comparison of W-cells with X- and Y-cells. J. Neurophysiol. 37:722-748

Straschill, M. and J. Perwein (1975) Effects of biogenic amines and amino acids on the cat's retinal ganglion cells. In M. Santini (ed): Golgi centennial Symposium. New York: Raven Press, pp. 583-591.

Valat, J., Privat, A., and Fulcrand, J. (1983) Multiplication and differentiation of glial cells in the optic nerve of the postnatal rat. Anat. Embryol. 167:335-346.

Vidal-Sanz, M., Villegas-Perez, M., Cochard, P., and Aguayo, A. (1985) Axonal regeneration from the rat retina after total replacement of the optic nerve by a PNS graft. Soc. Neurosci. Abstr. 11:254.

Wassle, H., Levick, W.R. and Cleland, B.C. (1975) The distribution of the alpha type ganglion cells in cat's retina. J. Comp. Neurol. 159:419-435.

Weinberg, E. and P. Spencer (1979) Studies on the control of myelinogenesis 3. Signalling for oligodendrocyte myelination by regenerating peripheral axons. Brain Res. 162:273-279.

Weiss, P. and A. Taylor (1946) Guides for nerve regeneration across gaps. J. Neurosurg. 3:375-389.

Wender, M., Koyik, M. and Goncerzewicz, A. (1981) Neuroglia in central Wallerian degeneration (ultrastructural and histoenzymatic studies). Journal Hirnforschung 22:205-216.

Wiesel, T. and D. Hubel (1963) Single-cell responses in striate cortex of kittens deprived of vision in one eye. J. Neurophys. 26:1003-1017.

Williams, L. and S. Varon (1984) Matrix modification enhances nerve regeneration within a silicone chamber. Soc. Neurosci. Abstr. 10: 1027.

Windle, W. (1956) Regeneration of axons in the vertebrate central nervous system. Physiol. Rev. 36:426-440.

Zalewski, A. and W. Silver (1980) An evaluation of nerve repair with nerve allografts in normal and immunologically tolerant rats. J. Neurosurg. 52:557-563.

Zeman, W., and J. Innes (1963) Craigies Neuroanatomy of the Rat. New York: Academic Press.